

STUDIES OF THE DYNAMICS OF MAGNETIZED
GRAVITATING DISK

by

B.P. PANDEY

A THESIS SUBMITTED FOR THE
DEGREE OF

DOCTOR OF PHILOSOPHY

OF THE
GUJARAT UNIVERSITY

B17606



043 PAN

NOVEMBER, 1989

पुस्तकालय THE LIBRARY
भौतिक अनुसंधान प्रयोगशाला
PHYSICAL RESEARCH LABORATORY
नवरांगपुरा, अहमदाबाद-380009.
NAVRANGPURA, AHMEDABAD-380009
भारत/INDIA


PHYSICAL RESEARCH LABORATORY
AHMEDABAD 380 009, INDIA

Dedicated to


All those upon whose smiles
my own happiness is fully dependent

Certificate

I hereby declare that the work presented in this thesis has not formed the basis for the award of any degree or diploma by any University or Institution.


B.P. Pandey
Author

Certified by:


Prof. R.K. Varma
Thesis Supervisor

Date: 17th November, 1989

CONTENTS

	<u>Page</u>
CHAPTER I : INTRODUCTION	1
1.1 : Historical Background	1
1.2 : Observational Techniques of Galactic Magnetic Field	6
1.2.1 : Optical Polarization	7
1.2.2 : Faraday Rotation	8
1.2.3 : Zeeman Effect	10
1.2.4 : Magnetic Field Strength from Equilibrium	11
1.3 : Earlier Theoretical Attempts	12
1.3.1 : Spiral Arms as Tubes of Force	13
1.3.2 : Helical Model	14
1.3.3 : Primordial Origin Theory	14
1.3.4 : Dynamo Theory	16
1.3.5 : Bisymmetric Spiral in a Small Thickness Disk	21
1.4 : Difficulties with Dynamo Theories	22
1.4.1 : Dynamos are Kinematical	22
1.4.2 : Time-Scale Problem	23
1.4.3 : Dynamos are Local	24
1.4.4 : Shortcomings of Sofue et.al's Treatment	25
1.4.5 : Shortcomings of Baryshnikova et.al's Treatment	25
1.4.6 : Feedback Problem	26
1.5 : Stability Analysis	26
1.5.1 : Hydromagnetic Stability of a Thin Self-Gravitating Disk	27

1.5.2	:	Effect of Poloidal Magnetic Field on the Stability of a Rotating Self- Gravitating Disk	30
1.6	:	Profile of the Present Studies	31
CHAPTER II	:	AN INFINITELY THIN MAGNETIZED PLASMA DISK IN THE GRAVITATIONAL FIELD OF THE GRAVITATIONAL BULGE - A SELF- CONSISTENT TREATMENT	34
2.1	:	Introduction	34
2.2	:	Magnetohydrodynamic Equations	36
2.3	:	Equilibrium for a Flat Disk	40
2.4	:	Normal Mode Analysis	45
2.5	:	Discussion	50
2.6	:	Variational Technique	54
2.7	:	A More General Treatment	58
2.8	:	Non-Dimensional Equations	62
2.9	:	Solution of Maxwell's Equations and Dispersion Relation	64
2.10	:	Global Eigenvalue Equation	68
2.11	:	Result and Discussions	76
CHAPTER III	:	NUMERICAL TECHNIQUES	81
3.1	:	Introduction	81
3.2	:	Construction of Eigen-Matrices	82
3.2.1	:	The Matrix Elements	83
3.2.2	:	Generation of Eigen Patterns	84
3.3	:	The Eigen Routine	85
3.4	:	Convergence of Eigen Values and Eigenfunctions	86

CHAPTER IV : EPILOGUE

88

REFERENCES

91

Acknowledgements

I have been fortunate to be associated with Professor R.K. Varma. I express my indebtedness for providing valuable guidance throughout the period of my work and introducing me to the fascinating field of plasma astrophysics.

I have been greatly benefitted by countless but useful* discussions with Professor J.C. Parikh. Professor Bimla Buti for her very "strict" reviewing of my basics (2nd year review) which has helped me enormously. Professor A.C. Das and Professor A.R. Prasanna for the very kind gestures and help during the long ups and down which is so common to this hazardous profession. Dr. B.R. Sitaram whose everreadiness and countless discussions have helped the author in many ways.

I express my deep sense of gratitude to the "human bondage" of Navin and Preeti, Bhushan, Anjan, Anindya and kailash whose love and affection has kept the author away from hundred years of solitude. Physics embedded in the warmth of friendship has been bestowed upon me selflessly by D.P.K. Banerjee, K.B. Vijaykumar, Dr. Sunil P. Rawat and Jitesh Bhatt. In a major way, they have influenced my scientific outlook, and I take this opportunity to express my gratitude.

It is a great pleasure to express my gratitude to Mr. P.S. Shah, Mr. M.S. Patel, Mr. G.N. Desai, Mr. G. Nathwani and Mr. S. Goel of Computer Centre for the help they have

rendered during the period of this work.

Everybody in the Library have been very kind and helpful and I take this opportunity to thank them all.

Most of the typing has been done by my friend Ravi Bhushan. I express my deep reverence for his selfless service rendered to me. Viswanathan has given the final touches to the manuscript and I express my gratitude to him.

Lastly, I am indebted to my wife without whose constant moral support this work might not have been possible.

B.P. Pandey

Abstract of the Thesis

The origin and maintenance of the galactic magnetic field have been studied in this thesis. Bisymmetric spirals are the most common feature of the magnetic field structure in the galaxies though some of them possess ring structure also. Even though dynamo theory explains the many observational features of the magnetic field of the galaxy, it remains unsatisfactory, on many counts.

Evolution of galactic magnetic field is related with the dynamics of the galactic plasma disk and hence it is necessary to find the "mechanism" which would contribute to the growth of the magnetic field in the galactic disk. We have studied here one such mechanism, which arises as a result of the non-uniformity of the matter density in the magnetized plasma disk. The inverted gradient of density column supported by plasma against the gravity is quite effective for the energy needed for the growth of the magnetic field. It is Rayleigh-Taylor instability which is responsible for the amplification of the magnetic field. It is found that such a process could amplify the magnetic field of the disk with the growth rates which depend on the density gradient of the matter etc.

A more complete theory of the bisymmetric spiral field, as the allowed eigen-functions of a gravitating magnetized disk would require a self-consistent solution as an eigenvalue problem with proper boundary conditions. We have

carried out such a study for a thin magnetized plasma disk with rigid rotation (which is the only permissible solution of the induction equation in the infinite conductivity limit). It is found that bisymmetric spirals appear as the allowed eigenmodes of the disks eventhough the disk is rigidly rotating which has to be contrasted with the differential rotations required for the dynamo action in the disk.

CHAPTER I

INTRODUCTION

1.1. Historical Background

The term "Galaxy" has been derived from the Greek word 'galaktokos' meaning milky. And the galaxy can be seen with naked eyes in the night sky as a pale, mysterious band of light of irregular brightness and width stretching across the heavens almost along a great circle. Edge-on view of the galaxy approximately resembles an enormous lens (Fig. 1) whose diameter is about 30 kpc ($1 \text{ pc} = 3 \times 10^{18} \text{ cm}$) with an average thickness of about 2 kpc. Two tightly twisted spiral arms (about 0.4 kpc) would be seen (Fig. 2) if viewed from

above.

Major contribution to the mass of the galaxy comes from the stars. The gas contributes only a few percent of the mass of the galaxy but it is responsible for the magnetic field of the galaxy (namely, the ionized component of the gas) and also for the birth of the new stars. By exploding and evolving, star returns the gas to the interstellar space. In addition to the gas, there is much dust in the galaxy. It is assumed that these dust particles are paramagnetic in nature.

Magnetic field of the Sun was discovered in 1908 by George Hale. Only after another 50 years the magnetic field of other stars were discovered by Harold Babcock and only during last two decades it became clear that magnetic fields are present around all stars.

Fermi (1949) was the first to propose that the disc of the galaxy contains a large-scale magnetic field. The first confirmation about the presence of the galactic magnetic field came in 1949 from the observations of star light polarization of distant stars by W.A. Hiltner. This polarization is due to the scattering of light by elongated dust grains aligned by the magnetic fields (Davis and Greenstein, 1951). For such an alignment would lead to different amounts of scattering of light polarized parallel and perpendicular to the magnetic field and, therefore, to a polarization of light reaching us. It can be shown (Spitzer, 1968) that for elongated particles, which one can idealize as prolate spheroids, a strong magnetic field B , can align

these grains so that their major axes tend to be uniformly distributed in a plane perpendicular to the magnetic field. If the magnetic field is perpendicular to the line of sight, the plane of vibration of the polarized light will then be parallel to B, since for E parallel to the orienting magnetic field the electric vector tends to be perpendicular to the major axis of the grains, and the extinction is less than for E perpendicular to B. Then, one expects to observe no polarization in the general direction of the magnetic lines of force, and maximum, in the perpendicular direction. And if one interprets from this point of view (Hiltner, 1951) the maps of polarization effects as a function of the direction of observation, one finds that the galactic magnetic field is roughly parallel to the direction of the spiral arms, in which we are located.

As one observes distant stars in a direction approximately perpendicular to the spiral arm, it appears that the direction of polarization plane is only approximately parallel to the arm i.e. the field lines are not straight but "wavy lines". The mean angular deviation of the plane of polarization from the direction of spiral arms is about $\alpha = 0.2$ radius (Hiltner, 1951). Chandrasekhar and Fermi (1953) concluded that there must be a relation between α and the magnetic field B. For a strong magnetic field, lines of force will be straight, whereas weak fields will be dragged in various directions by the turbulent motion of the gas masses in the spiral arm and α would be large.

The velocity of the transverse magnetohydrodynamical (MHD) wave is given by

$$V = \frac{B}{\sqrt{\mu \rho}}$$

where ρ is the density of the ionized matter. The ionized matter has a high electrical conductivity to be effectively attached to the magnetic lines of force in such a way that only longitudinal relative displacement are possible. Transverse oscillation of a particular line of force is described by

$$Y = a \cos k(x - Vt)$$

where x is the longitudinal coordinate and y is the lateral displacement. Now,

$$\frac{dy}{dx} = -ak \sin k(x - vt)$$

$$\frac{dy}{dt} = -akV \sin k(x - vt)$$

Where we see that

$$\left\langle v^2 \left(\frac{dy}{dx} \right)^2 \right\rangle = \left\langle \left(\frac{dy}{dt} \right)^2 \right\rangle$$

The lateral velocity of lines of force must be equal to the lateral velocity of the turbulent gas

$$\left\langle \left(\frac{dy}{dt} \right)^2 \right\rangle = \frac{1}{3} v^2$$

Factor $1/3$ arises from the fact that only one component of the velocity is effective in shifting the lines of force.

Hence,

$$\left\langle \left(\frac{dy}{dx} \right)^2 \right\rangle = \alpha^2$$

Therefore,

$$B = \sqrt{\frac{\mu \rho}{3}} \frac{v}{\alpha}$$

For our galaxy, $\rho = 2 \times 10^{-24} \text{ gm/cm}^3$, $v = 5 \times 10^5 \text{ cm/sec}$ and $\alpha = 0.2$ radians, so that

$$B = 7.2 \times 10^{-6} \text{ gauss}$$

Chandrasekhar and Fermi also derived the same order of magnitude value of the magnetic field by using the argument about the stability of the spiral arms. We know now that the arguments given by Chandrasekhar and Fermi about the stability of the spiral arms have been superseded. We present those arguments since they strongly influenced the development of galactic magnetic field theories. They equated the gravitational pressure in the spiral arm to the sum of the material and magnetic pressure and hence, concluded that the order of magnitude of above derived result is correct. As today we know from observations that this is the right order of magnitude of the field.

Observational data on the large-scale configuration of the galactic magnetic field started accumulating in mid-70s (Sofue et. al., 1986 and references therein). These data

provided the clear evidence of the alignment of the magnetic fields in the nearby galaxies. In contrast to the external galaxies local field in our galaxy has been extensively studied in the past few decades (King, 1983; Vallee, 1984). These data, namely on the Faraday rotation of the polarization plane by the ambient interstellar field has led to the conclusion that galactic magnetic field possesses two different kinds of morphologies - ring and bisymmetric spirals. Bisymmetric lines are directed inwards in one half of the galactic disc and outwards in the other (Fig. 3). Bisymmetric structure is most clearly seen in M33, it is also prominent in the nearby galaxies M51 (Fig. 4).

The majority of the spiral galaxies possesses bisymmetric spiral field (BSS), whereas only a minority such as M31 has a ring configuration. Table 1.1 (Sofue et al, 1986) summarizes the derived configurations studied so far together with their strength. Magnetic field structure of greater complexity than ring or bisymmetric spiral configuration are also expected to exist in these galaxies. But the observational accuracy is still too poor to reveal final structure except for the well studied local field in our galaxy.

1.2. Observational Techniques of Galactic Magnetic Field

An understanding of galactic magnetic field depends on independent type of observation and their interpretations, some of which apparently contradict each other. The

difficulty in the measurement of the field is caused by the enormous distance involved. Below we enlist briefly, different measurement techniques and difficulties involved with them.

1.2.1. Optical Polarization

The first evidence for interstellar magnetic field comes from measurements of optical polarization. The basic mechanism (as mentioned earlier) that is responsible for the optical polarization is the scattering of light by elongated dust grains aligned by the magnetic fields. Optical polarization measurements, however, give no field strength, only the orientation of the field. The field alignment is expected to be such that, the polarization vector E is parallel to the field orientation.

Davis and Greenstien first outlined the mechanism of optical polarization and the difficulties still being faced are that, it doesn't appear that interstellar field is strong enough to produce the necessary alignment, unless there are enhanced magnetic relaxation effects in the dust grain due to collective effects between adjacent iron atoms within grains producing either ferromagnetism or super-paramagnetism (Purcell & Spitzer, 1971).

The problem lies in the requirements for fields of several tens of microgauss for the simple Davis-Greenstien models, compared to few $\sim (3-5) \cdot 10^{-6}$ G known to exist in space, based on direct measurements. (See for review of the problem, Spitzer, 1978).

1.2.2. Faraday Rotation

As the radio waves propagates through some interstellar magnetoionic plasma, the polarization vector of some intrinsically linearly polarized continuum source (e.g. quasar) will be systematically rotated by the ambient magnetic field in the plasma. Amount of this rotation depends on the wavelength, the strength of the component of the magnetic field along the line of sight and the number of free electrons along the line of sight. Rotation angle is given by

$$\Phi = (RM) \lambda^2 + \Phi_0 \quad (1)$$

$$RM = 0.81 \int n_e B_{||} dl \quad (2)$$

where Φ is the rotation angle that determines the orientation of the polarization plane, n_e is the thermal electron density in cm^{-3} , $B_{||}$ is parallel component of the field along the path l from the source to the observer G ($g = 10^{-6} \text{ G}$), l is the path length in pc and Φ_0 is the intrinsic rotation angle in the source.

It has been pointed by Sofue et. al. (1985), that ring like and bisymmetric spiral structure produce different patterns of variation of the rotation angle Φ over the galaxy image. The ring configuration gives an odd dependence

of the rotation angle (and RM) on the distance along the major axis while the bisymmetric spiral configuration gives an even correspondence (Fig. 5). Difficulty with rotation angle measurement stems from the fact that Φ cannot be determined uniquely since for any Φ , $\Phi + n\pi$, $n = 1, 2, \dots$ is also a solution. For example, position angle measurement of NGC 2903 seems to fit an even dependence (solid line in Fig. 6). However, addition of 180° to the angle at the right side of the plot allows an equally successful interpretation of these data (dashed line, Fig. 6) (Ruzmaikin et. al., 1986). This difficulty can be removed by taking multifrequency observations (Ruzmaikin and Sokoloff, 1979).

Faraday rotation measurements in our galaxy show that the large-scale magnetic field probably changes sign in every spiral arm, from Perseus to Sagittarius (Ruzmaikin et al., 1986). However, the investigated region (Fig. 7) is very small (~ 3 kpc) as compared to the overall dimension of the galaxy (~ 15 kpc) and conclusions about the global magnetic field seems to be premature. Available data cannot distinguish bisymmetric structure from a ring with alternating fields. In many cases decisive evidence exists on magnetic field structures (Sofue and Takano, 1981; Beck, 1982).

Another difficulty is due to the fact that Faraday rotation can take place within the source itself, where the radiation is generated (Zeldovich et. al., 1983). This may result in the violation of the simple law (1), relating the type of radiation to the source structure (Ruzmaikin and

Sokoloff, 1979; Vallee, 1980).

1.2.3. Zeeman Effect

In the absence of external magnetic field, atomic energy levels are degenerate. Magnetic field removes the degeneracy. The energy level splits, each energy level being defined by the conserved projection of the total angular momentum, on the field direction B . The splitting of energy level leads to a corresponding splitting of spectral line of an emitting or absorbing atom.

In the simplest case, when Lande factor g (which allows especially for the spin and is equal to one for an atom with total zero spin) is the same for the upper and lower energy levels, the line is split into a triplet

$$\nu_{\pi} = \nu_0 \quad ; \quad \nu_{\sigma} = \nu_0 \pm g \left(\frac{e}{4\pi m c} \right) H$$

(normal Zeeman triplet). The unshifted π -component corresponds to a transition that leaves the projection of total angular momentum unchanged. It is linearly polarized while symmetric σ -components correspond to the transitions in which projection of total angular momentum in the field direction changes by ± 1 and have, respectively, right-handed and left-handed circular polarization.

Direct measurement of the interstellar magnetic field is done using Zeeman effect. In HI (or OH) radio lines, in a magnetic field, Verschuur (1974, 1979) has observed the Zeeman effect in dense interstellar cloud in the galaxy. In external galaxies, this type of observation has not been

made. Main difficulty in using this effect stems from the fact that Doppler broadening significantly exceeds the Zeeman splitting. For a 21 cm hydrogen line, the distance between the σ -components is

$$\Delta\nu \approx 2.8 \times 10^6 B \text{ Hz}$$

while the Doppler width of the line is 20 KHz (Kaplan and Pikelner, 1970).

1.2.4. Magnetic Field Strength from Equipartition

It is assumed that there is an equipartition of energy density between the cosmic rays and magnetic field. Also the electron in the relevant range of energies has an isotropic velocity distribution and a differential energy spectrum of the form

$$N(E)dE = N_0 E^{-\gamma} dE$$

In order to relate the electron fluxes at the source and the Sun, it is assumed that these values are the same i.e. N_0 is uniform throughout the galaxy. According to guiding centre approximation (magnetic moment - adiabatic invariant), N_0 is uniform and velocity distribution is isotropic all along the line of force (reflection at higher B is compensated by increased density of the field lines).

Magnetic field energy is $\frac{B^2}{2\mu}$. From equipartition

$$\frac{B^2}{2\mu} = a \int_{E_1}^{E_2} E N(E) dE$$

where E_1 and E_2 are relevant energies, corresponding to the lower and upper cutoff frequencies ν_1 and ν_2 of synchrotron radio spectrum. a is the ratio of total cosmic ray energy to the electron energy. B (in G) is given by

$$B = (2.3) (aE\xi)^{2/7}$$

where ξ is the volume emissivity ($\text{ergs}^{-1} \text{cm}^{-3}$) and A is given by

$$A = C \left(\frac{\alpha+1}{\alpha+\frac{1}{2}} \right) \left(\frac{\nu_2^{\alpha+\frac{1}{2}} - \nu_1^{\alpha+\frac{1}{2}}}{\nu_2^{\alpha+1} - \nu_1^{\alpha+1}} \right)$$

where $C = 1.057 \times 10^{12}$ in cgs and $\alpha = -(\delta-1)/2$ - radio spatial index. Emissivity is given by

$$\xi = \frac{4\pi}{\ell} \int_{\nu_1}^{\nu_2} I_\nu d\nu$$

I_ν is the intensity and ℓ is the path length.

Equipartition hypothesis is open to objections but the magnetic field strength calculated for external galaxies is in good agreement with the values, found by other methods.

1.3. Earlier Theoretical Attempts

It is often found that usual hydrodynamics is incapable of describing astrophysical phenomenon without including

the electromagnetic effects, since almost all phenomena of astrophysics occur when there are magnetic fields associated with material of large conductivity and hence a strong coupling results between the motion of matter and the magnetic field. Motion of the highly conducting matter in the magnetic field induces an electric field, perpendicular to both the magnetic field and the motion of the matter. This gives rise to current, which acts back on the moving matter. This is how the coupling takes place between the moving matter and the magnetic field.

Magnetic field in the astrophysical situations are the offspring of the above mentioned magnetohydrodynamical motions. Below, we briefly introduce the earlier theoretical attempts to explain the magnetic field.

1.3.1. Spiral Arms as Tubes of Force

Chandrasekhar and Fermi (1953) were led to postulate the existence of a magnetic pressure opposing the gravitational contraction of the arm from the comparison of the dynamical and gravitational energies of the arm. Dynamical energy of the gaseous material inside the arm is $\sim 1.25 \times 10^{11}$ erg/gm, for a random velocity $v \sim 5$ km/s. Gravitational potential, between the central axis and the surface of an arm $\sim Gm = 8 \times 10^{11}$ erg/gm for m (gas+star) $\sim 1.2 \times 10^{19}$ gm. Therefore, if dynamical motion balances the gravitation, the dynamical energy has to be $\sim 0.5 Gm$. In fact, gravitational energy appears to be six times greater than the dynamical energy. Therefore, magnetic pressure should

also be taken into consideration.

Model of Chandrasekhar and Fermi is not correct in the light of observations which became available only after 1960's. Spiral arms are mainly caused by the density wave (Lin and Shu, 1964) and they are not the tubes of force as thought by them.

1.3.2. Helical Model

To overcome the difficulty of the "cylindrical" model of Chandrasekhar and Fermi, Hoyle and Ireland (1959) proposed that magnetic field lines are helices wound around the axis of the spiral arm. It is assumed that the magnetic lines pass through or near the galactic center. There they become twisted. As the gas and twisted field move out into the plane, the helix follows.

It is also assumed that halo field possesses large scale regularity. Halo lines of force are crossing the plane through the inter arm region. The lines of force are frozen in the halo as well as in the disk.

Major difficulty of this model is the way, halo field lines are connected through the interarm region from the opposite side of the plane. This model assumes that halo field lines are at first connected with the surrounding arms from near the center, then they are convected radially across the plane with the arms and then they are disconnected when arriving at the edge of the plane.

1.3.3. Primordial Origin Theory

In this theory, it is assumed that a uniform intergalactic field ($\sim 10^{-9}$ G) was captured by a protogalaxy (Fig. 8). Gravitational collapse of the protogalaxy took place and owing to the angular momentum conservation in the collapse, the uniform intergalactic field was, thus, twisted by the differential rotation into a bisymmetric spiral configuration (Fig. 9) and maintained upto the present time by some "mechanism" (Piddington, 1964; 1978).

Differential rotation will cause an overwinding of the field lines and to avoid that, a "mechanism" was proposed by Sawa and Fujimoto (1980). They assumed that the disk field is transported randomly by interstellar turbulence and diffuses outward across the surface of the galactic disk. They also assumed that the magnetic field of the halo can simultaneously diffuse back in the disk. Then the field lines in the disk are in open spiral configuration without being twisted by the differential rotation. The steady-state configuration is considered to be achieved by this kind of arrangement. The tightly twisted field lines in the disk are transported by the turbulent motion of the interstellar gas up into the halo, where the magnetic energy is relatively large enough to relax their tight winding since the field strength in the halo is comparable or slightly less than that in the disk $(2-3) \times 10^{-6}$ G (Sofue et. al., 1979). The less twisted lines of the halo diffuses into the disk across its upper and lower surface and they are twisted and strengthened again by differential rotation.

In addition to being kinematical in nature, the theory of Sawa and Fujimoto and Fujimoto and Sawa requires a halo field of the order of or slightly less than the disk field. There is no consensus as yet on the strength of the halo magnetic field other than that it is $\sim 10^{-6}$ G.

Kulsrud (1986) has suggested a model of the field which avoids the winding up dilemma without using the turbulent diffusion. One knows that in a weakly ionized plasma, ambipolar diffusion (i.e. relative drift between ions and neutrals) allows hydromagnetic forces to act on the neutrals through friction. If the interstellar gas above the galactic plane is partially supported by the magnetic fields then there must be a drift of the field lines away from the galactic plane, which ~ 0.04 km/s. This velocity moves the lines upward by one to two scale heights over 10^{10} year.

1.3.4. Dynamo Theory

G. Larmor in 1919 suggested that the magnetic field of earth and the Sun is generated by the hydrodynamic motion of the fluid. Dynamo theory went through several phases of development (for a detailed account, see Parker, 1979).

Essential features of the dynamo mechanism in the gaseous disk are:

- a. disk rotates non-uniformly causing a shear given by

$$G \equiv \frac{dV_0}{dr} - \frac{V_0}{r}$$

where V_0 is rotational velocity.

b. turbulence in the disk is cyclonic, i.e. local angular velocity of the gas in the disk causes the small eddies in the fluid.

c. the first stage of the galactic dynamo process is differential rotation. Non-uniform rotation of spiral galaxies turns a purely meridional field into one which is a combination of meridional and azimuthal components. The angular velocity of the gas is higher at the smaller radii, and a meridional field (fig. 10) is stretched into a trailing spiral.

The feedback loop of the galactic dynamo is associated with the cyclonic turbulence. A turbulent cell, rising through the disk expands because the density scale height of the interstellar gas slightly exceeds the correlation scale of the turbulence. The coriolis force from galactic rotation delivers an additional rotation to the expanding cells. Descending cells contract and acquire an oppositely directed coriolis rotation, but all cells above (or below) the galactic plane have helicity ($\underline{v} \cdot \nabla \times \underline{v}$) of the same sign (fig. 11). The mean helicity $\langle \underline{v} \cdot \nabla \times \underline{v} \rangle$ where $\langle \dots \rangle$ is an ensemble average, is thus an odd function of the vertical coordinate z , and breaks the mirror symmetry of the plane. The average deviation from reflection symmetry in the presence of an azimuthal field results in emergence of a mean meridional magnetic field.

The action of helical turbulence is equivalent to the generation of an azimuthal electromotive force αB_ϕ where α is a function of position and is proportional to the

mean helicity of the turbulence. Therefore, induction equation, when averaged over turbulent pulsation acquires an additional term. Basic induction and dynamo equations are (Baryshnikova et. al., 1987):

$$\frac{\partial \underline{B}}{\partial t} = \nabla \times \underline{v} \times \underline{B} + \beta \nabla^2 \underline{B} + \nabla \times (\alpha \underline{B}) \quad (3)$$

$$\nabla \cdot \underline{B} = 0 \quad (4)$$

where $\underline{B} = \langle \underline{B} \rangle$, \underline{v} is the regular velocity and $\alpha = -\tau \langle \underline{v} \cdot \nabla \times \underline{v} \rangle$ with τ the correlation time and \underline{v} the turbulent velocity.

Induction and dynamo equation for a thin, differentially rotating disk of finite thickness was solved by Parker (1971a, b, 1975) as an eigenvalue problem for axisymmetric mode. Below we briefly describe the treatment given by Sofue et al (1986). Galactic rotation \underline{u} is assumed to have only azimuthal component, i.e. $\underline{u} = (0, V(r), 0)$ and $\underline{B} = (B_r(r, z), B_\varphi(r, z), B_z(r, z))$ in (r, φ, z) coordinates in which all components are independent of φ . Writing equation (3) in local rectangular coordinate (x, y, z) whose origin rotates with the disk in the matter, and taking α as a pseudo-scalar (generally speaking the mean helicity is a pseudo-tensor α_{ik}). In real astrophysical disks, however, the turbulence is usually of small scale i.e. the mixing length is less than the disk thickness and hence almost isotropic. Therefore, $\alpha_{ik} = \alpha \delta_{ik}$ approximately, where α is a pseudo-scalar (Zeldovich et. al., 1983)), we have

$$\frac{\partial B_x}{\partial t} = \beta \left(\frac{\partial^2 B_x}{\partial x^2} + \frac{\partial^2 B_x}{\partial z^2} \right) + \frac{\partial}{\partial z} (\alpha B_y)$$

$$\frac{\partial B_y}{\partial t} = \beta \left(\frac{\partial^2 B_y}{\partial x^2} + \frac{\partial^2 B_y}{\partial z^2} \right) + \frac{\partial V}{\partial x} B_x$$

$$\frac{\partial B_z}{\partial t} = \beta \left(\frac{\partial^2 B_z}{\partial x^2} + \frac{\partial^2 B_z}{\partial z^2} \right) - \frac{\partial}{\partial x} (\alpha B_y)$$

$$\frac{\partial B_x}{\partial x} + \frac{\partial B_z}{\partial z} = 0$$

where x is directed away from the center, y -axis is parallel to the direction of galactic rotation and z -perpendicular to the disk.

A solution of the form $B = b \exp(-i\omega t + k_x x + k_z z)$ is substituted in the above equations and one gets the dispersion relation

$$\left(\frac{k_x^2}{k^2} + \frac{k_z^2}{k^2} - \frac{i\omega}{\beta k^2} \right)^2 - \frac{i k_z}{k} = 0$$

where $k = 3 \left(\frac{G \alpha}{\beta^2} \right)^{1/2}$ with $G = \left(\frac{dv}{dx} - \frac{v}{x} \right)$. If one assumes that $k_x = p$ then the dispersion relation is reduced to the relation between ω and k_z . One has four roots of the above equations $k_z(n_1, n_2, n_3, n_4)$. Therefore, the general solution can be represented as a superposition of 4-plane waves

$$\underline{B} = \sum_{j=1}^4 \underline{b}_j \exp \left[i(-\omega t + px + n_j z) \right]$$

From the boundary condition, the magnetic field suffers a discontinuity across the plane, i.e.

$$\left. \frac{\partial B_{x,y}}{\partial z} \right|_{|z|=0} = 2\alpha B_x B_y (z=0)$$

one determines ω and amplitude b_j ($j=1, 2, 3, 4$) as an eigenvalue problem. Local ring field results as a solution (Sofue et. al., 1986).

Induction and dynamo model for a ring field was extended by Sawa and Fujimoto (1986) and Fujimoto and Sawa (1986) for the bisymmetric spiral fields. Bisymmetric spiral field, contrary to the ring fields depends on azimuthal angle also.

Since magnetic field possesses a spiral structure, solution is searched in the form

$$\underline{B} = \underline{b}(r) \text{Exp} \left[i(-\omega t + \varphi + k_2 z + \ln \frac{r}{\delta}) \right]$$

where $\underline{b}(r)$ varies slowly with radius. $\varphi + \ln r/\delta = \text{const}$, describes the spiral and hence its presence in the exponential.

Plugging it in the induction and dynamo equation, with the expansion of $\underline{b}(r)$ in

$$\underline{b}(r) = \underline{b}_0(r) + \underline{b}_1(r)\delta + \underline{b}_2(r)\delta^2 + \dots$$

and taking only the dominant terms, one gets a dispersion relation for the BSS field

$$\left(\frac{1}{R^2 r^2 \delta^2} + \frac{k_2^2}{R^2} + \frac{iV}{\beta R^2} - \frac{i\omega}{\beta R^2} \right)^2 - \frac{i k_2}{R} = 0$$

where

$$k = \left(\frac{G_1 \alpha}{\beta^2} \right)^{1/3} ; \quad G_1 = \frac{dv}{dr} - \frac{v}{r}$$

This dispersion relation gives four roots for k_z against ω . Thus the general solution is superposition of 4 spiral waves

$$\underline{B}(r, \varphi, z) = \sum_{j=1}^4 \underline{b}_j(r) \text{Exp} \left[i(-\omega t + \varphi + n_j z + i n_j^2 r^2) \right]$$

b_j and ω are determined through an eigenvalue problem.

Sawa and Fujimoto have found that the region of local maximum field traces two spirals on the galactic plane and that the magnetic field reverses its direction across the boundary of the two spirals. Therefore, they concluded that induction and dynamo process is responsible for the bisymmetric spiral magnetic field.

1.3.5. Bisymmetric Spirals in a Small Thickness Disk

Kinematic dynamo problem in the small thickness disk (i.e. $\lambda \ll 1$, where, λ = height of the disk/radius of the disk) has been considered by Baryshnikova et.al. (1987, c.f. also Ruzmaikin et. al., 1981, 1985).

They considered an axisymmetric disk (the coefficients in (3) do not depend on φ). Normal mode of the dynamo equation (3) have the form

$$B = B(r, z) \text{Exp}(\Gamma t + i m \varphi)$$

Equation for B_z splits up from equation (3) in the leading orders and equation (3) can be solved autonomously for B_r and B_φ .

In the thin disk, solution of equation (3) for B_r and B_φ can be constructed in the following way.

$$\begin{bmatrix} \tilde{B}_r \\ \tilde{B}_\phi \end{bmatrix} = Q(r) \begin{bmatrix} b_r(r, z) \\ b_\phi(r, z) \end{bmatrix}$$

Where, b_r and b_ϕ depend parametrically on radius and satisfies the local dynamo equation. If one puts $\frac{\partial b_r}{\partial r} = 0$ and $\frac{\partial b_\phi}{\partial r} = 0$ (this is the essence of the approximation used, since $\frac{\partial}{\partial r} \rightarrow 0$) in equation (3) for B_r and B_ϕ components, one gets a Schrodinger equation with a complex potential.

$$\lambda^2 \frac{d}{dr} \left[\frac{1}{r} \frac{d}{dr} (r Q) \right] - U(r) Q = P Q$$

$$U(r) = -\gamma(r) + im R_\omega \omega \quad (5)$$

When the radial potential $U(r)$ is determined from local generation problem, equation (5) gives the growth rate (eigenvalue) and radial field distributions $Q(r)$ (eigenfunctions).

It should be noted that major problem that arises in this model is similar to the other dynamo models i.e. it is a local theory. One knows that magnetic fields are global features of the galaxies and therefore, a global eigenvalue problem must be solved, if this model were to explain the observed magnetic field structures in the galaxies.

1.4. Difficulties with Dynamo Theories

1.4.1. Dynamos are kinematical

Main problems of the dynamo theories are to construct a velocity field capable of indefinite maintenance and

amplification of an initially given field. Source of energy for maintaining the magnetic field is derived from the plasma fluid and is not self-consistent with the ultimate source of energy, namely, the gravitational field. In this sense these theories are kinematical. Therefore dynamo theory is an incomplete theory of magnetized matter and its interactions with the magnetic field in presence of the gravitational field of the galactic bulge.

1.4.2. Time-scale Problem

Assuming the thickness of the ionized galactic layer h to be ~ 400 pc (in agreement with the observed pulsar dispersion measure, Zeldovich et. al., 1983) and magnetic diffusion constant $\beta \sim 10^{26}$ cm²/s the field has to grow faster than the characteristic diffusion time

$$\gamma = 1/t = h^2/\beta \sim 5 \times 10^8 \text{ yr} \sim (1/20) \times \text{age of the galaxy}$$

We know that $B < B_{\max} = B_0 \exp(\gamma t)$. For the dynamo to act, one needs an initial seed field to be amplified and changed. In the case of planets and stars question about the seed field is not asked since it is assumed that weak fields always exist in the medium in which these objects are formed. But in the case of Galactic dynamo, no evidence exists of appreciable intergalactic magnetic field. Assuming the above mentioned growth time of the Galactic dynamo, during the period of the Galaxy's existence ($\sim 10^{10}$ yrs), the observed field ($\sim 2 \times 10^{-6}$ G) could be produced by an

initial field of $\sim 10^{-21}$ G.

Above argument has a flaw for the following reasons. Even though dynamo ($\alpha - \omega$) type gives the exponential growth rate of the magnetic field $\exp(\Gamma t)$, $B = B_0 \exp(\Gamma t)$ to go from 10^{-21} G (a maximal seed field) (Harrison, 1970) to 10^{-6} G one needs 40 exponential foldings (since $T_{\text{dynamo}} \sim 2 \times 10^8$ yr).

Taking the life time of a typical galaxy to be $\sim 10^{10}$ year, radius to be of the order of ~ 20 Kpc, flat rotation curve with a velocity ~ 200 km/s, one gets the rotation frequency $\sim 10^{-8}$ /yr. Since formation of the galaxy, the number of revolution required, can be estimated from

$$10^{-6} \text{ G} = (10^{-21} \text{ G}) \times \text{Exp}(20-40)$$

Therefore, one needs 20-40 revolutions to amplify a weak seed field. This means that galaxy barely had time to amplify a weak cosmic seed field. At redshift of the order of 3-4 when the age of the galaxy is $\sim 10^9$ and 10^8 yrs respectively, galaxies will not have time to spin even once and thus required amplification factor will not be achievable i.e. observed magnetic field of the order of 10^{-6} G at $z=3-4$ cannot be made by the galactic dynamo mechanism (Norman, 1987).

1.4.3. Dynamos are local

For the generation of the dynamo action in the galactic disk, finite resistivity of the fluid is required ($\beta \neq 0$). In

almost all the astrophysical situations resistivity is taken to be zero owing to the large scale length involved. Magnetic Reynold number, which measures the role of the ionized gas motions relative to the magnetic diffusion is given by

$$R_m = \frac{VL}{\beta}$$

where V is the fluid velocity, L - typical scale length and β - coefficient of magnetic diffusion. For the interstellar environment, taking $v = 10$ km/s, $L = 100$ pc and $\beta \sim 2 \times 10^{21}$ cm²/s one gets $R_m = 5 \times 10^4$. This high value of Reynold number indicates that magnetic diffusion is negligible compared to the ionized gas motion and that the diffusion can only be considered for the scale-heights below $10^{-1} 10^{-2}$ pc. For a dynamo to work, one knows that a finite resistivity is required (Ruzmaikin et. al., 1988) and therefore, dynamo action can be invoked locally only. Magnetic fields of the galaxies are a global feature and therefore, dynamo theories do not carry the conviction over large scale.

1.4.4. Shortcoming of Sofue et. al.s Treatment

In addition to the general difficulties of the dynamo theories, as pointed above, the dynamo theory of Sofue et al assumes the solution of the dynamo equation as the spiral waves locally. Bisymmetric spiral should follow as the dynamical consequence of the theory and therefore, dynamo theory of Fujimoto et al lacks conviction.

1.4.5 Shortcoming of Baryshnikova et. al.s treatment

Most of the galaxies possesses bisymmetric spiral fields. Therefore, one would expect that the preferred mode in the galactic disk would be lowest non-axisymmetric mode. Growth rate predicted by dynamo model of Baryshnikova et. al. predicts smaller growth rate for $m=1$ mode. The dominant mode in the dynamo's are axisymmetric. Introducing modulation of axisymmetric disk by spiral arms through $\cos(n\varphi)$ ($n \geq 2$, corresponding to number of spirals in the galaxies) and also by tidal interaction by nearby galaxies, Krasheninnikova et. al. (1989) have at least brought the growth rate for $m=1$ mode closer to $m=0$. That means in the galaxy the number of ring and bisymmetric morphology should be equally distributed which is not supported by observations.

1.4.6 Feedback Problem

All the dynamo theories suffer from this problem. Feedback of magnetic field on the fluid is assumed to be negligible. Energetic arguments (Zweibel, 1987) suggest that this is not the case. Feedback has been shown to be very important in models of the solar dynamo (Gilman, 1983).

1.5. Stability Analysis

One knows from the observations that ionized gas component constitutes 3 to 4% of the total gas content in the galactic disc. Therefore, the study of the magnetic field on the dynamics of the system is of interest. Stability

analysis of a magnetized disc is of great importance for the evolution of the magnetic field itself.

The effect of the magnetic field on the dynamics of the galaxy has been studied by several authors. Below, we enlist some of them.

1.5.1. Hydromagnetic stability of a thin self-gravitating disk (Hosking, 1969).

The stability of a thin, differentially rotating magnetized, self-gravitating cold disk is considered. The dynamics of the disk is described by the following MHD equations (in cylindrical r, φ, z coordinate), valid for $z=0$.

$$\frac{\partial \sigma}{\partial t} + \frac{1}{r} \left[\frac{\partial}{\partial r} (r \sigma v_r) + \frac{\partial}{\partial \varphi} (\sigma v_\varphi) \right] = 0 \quad (6)$$

$$\sigma \left(\frac{\partial \underline{v}}{\partial t} + \underline{v} \cdot \nabla \underline{v} \right) = \sigma \nabla \phi + \underline{j} \times \underline{B} \quad (7)$$

$$\frac{\partial \underline{B}}{\partial t} = \nabla \times \underline{v} \times \underline{B} \quad (8)$$

and Maxwell's equation :

$$\begin{aligned} \nabla \cdot \underline{B} &= 0 \\ \nabla \times \underline{B} &= \mu_0 \underline{j} \delta(z) \end{aligned}$$

Where $\sigma(r, \varphi, t)$ is the surface mass density of the gas,

$\underline{v}(r, \varphi, t) = (v_r, v_\varphi, 0)$ is its material velocity,

$\phi(r, \varphi, z, t)$ is the negative of the gravitational potential, $\underline{j} = (j_r, j_\varphi, 0)$ is the surface current density and $\underline{B}(r, \varphi, 0, t)$ is the magnetic field.

First equilibrium with an azimuthal current was considered. With $\underline{v} = (0, v_\varphi, 0)$, $v_\varphi = r\Omega(r)$,

$$\phi = \phi_0(r, z), \quad \underline{B} = (B_r, 0, B_z)$$

Equation of motion (7) can be written as

$$-r\Omega^2 = \left(\frac{\partial \phi_0}{\partial z} \right)_{z=0} + j_{0\varphi} B_z$$

$$0 = \left(\frac{\partial \phi_0}{\partial z} \right)_{z=0}$$

Perturbing over the above equilibrium, linearizing the MHD equations (i.e. retaining first order term only) and expressing the time dependence as $\exp(i\omega t)$ and φ dependence as $\exp(im\varphi)$ and applying WKB approximation one gets the following dispersion relations.

$$\omega_i^2 - (\omega_i - m\Omega)^2 + k^2 - \left(\frac{2\pi G \sigma_0}{R} \right) k - \left(\frac{B_z^2}{2\pi \sigma_0} \right) k = 0 \quad (9)$$

$$\left(\frac{m j_{0\varphi} B_z}{4\pi \sigma_0} \right) k - 2\omega_i (\omega_i - m\Omega) = 0 \quad (10)$$

where, $R = \frac{\sigma_1}{\sigma_{1, \text{total}}}$ is the gas fraction of total self-gravitating mass, G -gravitational constant, and

$$k^2 = \left[4\Omega^2 \left\{ 1 + \left(\frac{r}{2\Omega} \right) \frac{d\Omega}{dr} \right\} \right]_{r=R}$$

Where, R is the reference radius.

The growth rate of the instability is the negative root of

$$2\omega_i^2 = \left(\frac{2\pi\sigma_0}{R} k - k^2 - \frac{B_z^2}{2\pi\sigma_0} k \right) + \left\{ \left(\frac{2\pi G\sigma_0}{R} k - k^2 - \frac{B_z^2}{2\pi\sigma_0} k \right)^2 + \left(\frac{\mu_0 J_{0\varphi} B_z}{4\pi\sigma_0} k \right)^2 \right\}^{1/2}$$

which exists for all the radial wave number k . In particular there is instability at wavelengths that are neutrally stable according to gas-dynamical theory.

When equilibrium current is radial, i.e. initial equilibrium state is described by $\sigma = \sigma_0(r)$, $v_r = 0$, $v_\varphi = r\Omega(r)$, $J_r = J_{0r}(r)$, $\underline{B} = (0, B_\varphi, 0)$

From $\frac{d}{dr}(rJ_{0r}) = 0$ one has

$$J_{0r} = \frac{M}{r}$$

where, the constant may be considered to be the strength of a current source located at $z=0$. Reference to Maxwell's equation shows that

$$-\frac{\partial B_\varphi}{\partial z} = \mu_0 J_{0r} \delta(z)$$

and

$$r^{-1} \frac{\partial}{\partial r} (r B_\varphi) = 0$$

From where,

$$B_\varphi = -2\mu_0 J_{0r} \operatorname{sgn} z$$

The nontrivial linear perturbation equation at $z=0$, derived from (8) is

$$\dot{\lambda} (\omega - m\Omega) \tilde{B}_z = 0 \quad z=0$$

Where, use has been made of the fact that B_r and B_ϕ suffers a discontinuity at $z=0$.

It follows that one has to solve equation (6) and

$$\frac{\partial \underline{v}}{\partial t} + \underline{v} \cdot \nabla \underline{v} = \nabla \phi$$

on $z=0$ together with Poisson's equation for gravitational potential ϕ . The problem reduces to purely gas-dynamic one treated by Lin & Shu(1964).

Stability analysis considered by Hosking is not self consistent since Ohm's law (equation(8)) has not been considered properly. On the one hand, while the differentially rotating equilibrium disk assumed by Hosking would be inconsistent with the equilibrium Ohm's law, the Ohm's law is nevertheless considered for the stability analysis. No justification is offered by Hosking for such an apparent inconsistency.

1.5.2 Effect of Poloidal Magnetic Field on the Stability of a Rotating Self-Gravitating Disk

A stability analysis of an isothermal, rotating, magnetized equilibrium disk has been carried out by Nakamura (1983, 1984). Equilibrium state consists of Spitzer's(1942) density distribution $\rho_0(z)$ which is assumed to rotate rigidly. The disk is threaded by a uniform magnetic field $\underline{B} = B_0 \hat{z}$. The equilibrium in the radial

direction is not due to forces but due to the homogeneity in this direction.

In this model, the physical equilibrium quantities are unrelated. There is no equilibrium condition in the r -direction. Therefore, it's not a correct model.

Schmitz(1987) investigated the behaviour of a rotating self-gravitating equilibrium configuration with inhomogeneous magnetic field and pressure gradient in the radial direction. Rotational velocity is consistent with the Ohm's law (equation(10)). The stability of the system is investigated by the use of marginally stable axisymmetric perturbation.

Schmitz's stability analysis is not correct since erroneously, he has dropped the radial component of the Ohm's law and then wrongly concluded that radial magnetic field doesn't enter the equation of motion.

1.6. Profile of the Present Studies

From the above discussion it is clear that while dynamo theories have been made to fit observational bisymmetric spiral patterns, they are incomplete and not quite consistent from a theoretical standpoint.

A conducting medium moving across the magnetic field induces an electric field which generates a current and this in turn modifies the field, which in turn modifies the motion of the fluid, the fluid motion itself is being modified by gravitational field. Therefore, a complete theory

of the interaction of the magnetic field and ionized gravitating galactic matter must be considered self-consistently as an eigenvalue problem for the perturbation of the equilibrium disk with a given current density distribution. Solution of Maxwell's equations the magnetic field, inside the disk should be matched with the solution outside. The system will, in general, furnish complex but discrete eigenvalues for the frequency of the magnetic field perturbations, the real part of which will be related to the pattern velocity of the spiral and imaginary parts will give the growth rate. The corresponding eigenfunctions would furnish the eigen-patterns in the disk for the perturbation.

It is clear that this proper solution of the problem, as outlined here, will automatically obviate the difficulties (1.4.1, 1.4.3-1.4.5) pointed out above because they relate, in one form or the other, to the absence of a proper self-consistent solution of the problem in dynamo theories.

The large scale primordial cosmic magnetic field which one needs in magnetohydrodynamical treatment of the problem is $\sim 10^{-9}$. Growth of this primordial field should be caused by some instability in the disk.

In Chapter II, first we investigate the eigenvalue problem for an inviscid, incompressible, infinitely conducting fluid for which Rayleigh-Taylor mode is derived. Dispersion relation is recast in the variational form and we have obtained the axisymmetric solution. Next, we study numerically the allowed eigenmodes of a magnetized gaseous

disk with a general equation of state as an eigenvalue problem with appropriate boundary condition. The natural, discrete eigenvalues and corresponding eigenfunctions have been obtained with $m = 1, 2$. The magnetic field perturbations have been plotted in 3D form to show the allowed pattern in the disks for a number of radial wave numbers.

Chapter III introduces briefly the numerical methods used in the study of the global modes in the disk. The stability and reliability of the results are discussed.

Finally, in Chapter IV, we discuss the salient features of the present study and also future directions.

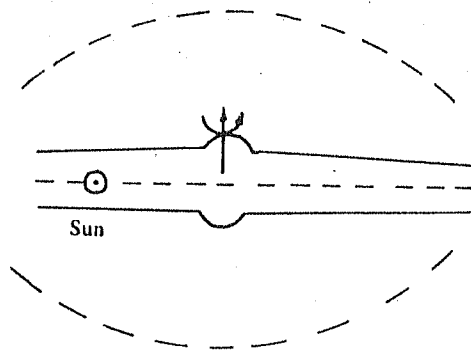


Fig. 1

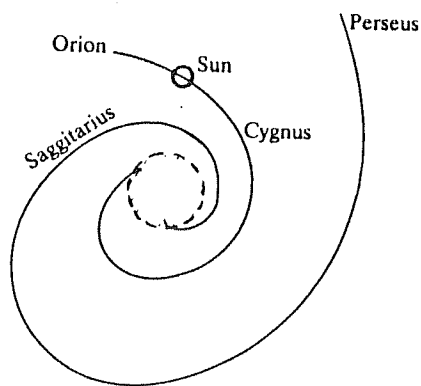


Fig. 2

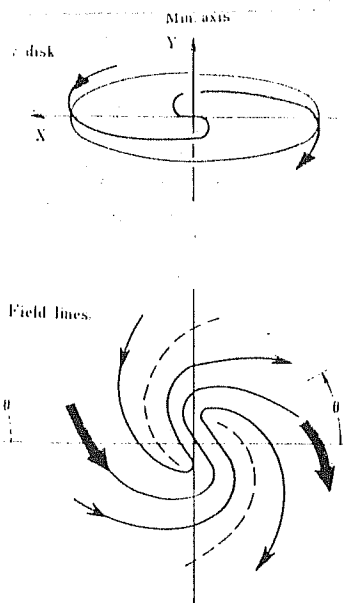


Fig. 3

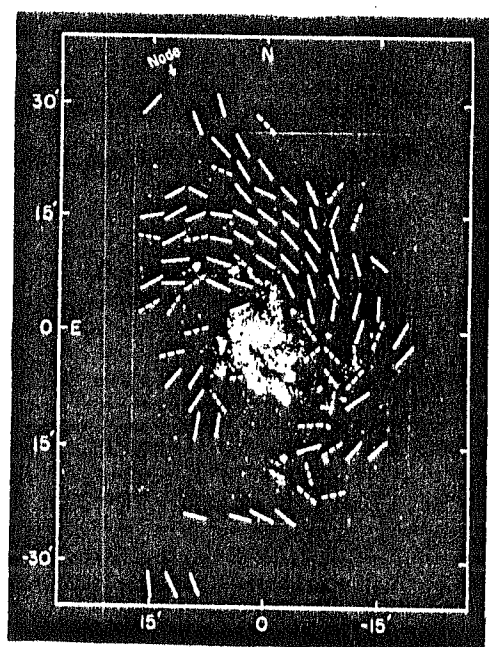


Fig. 4

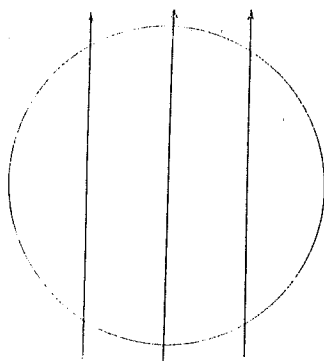


Fig. 5

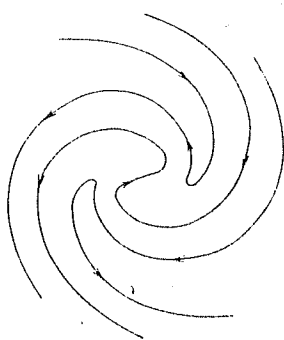


Fig. 6

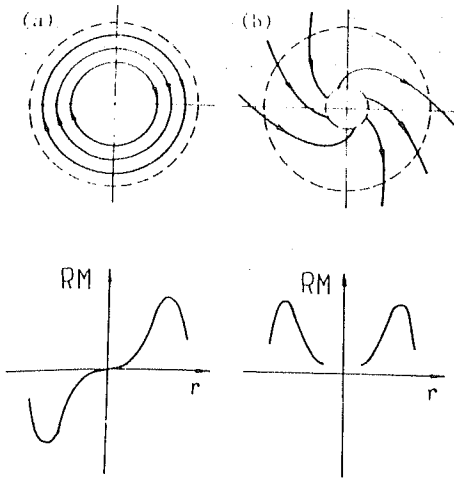


Fig. 7

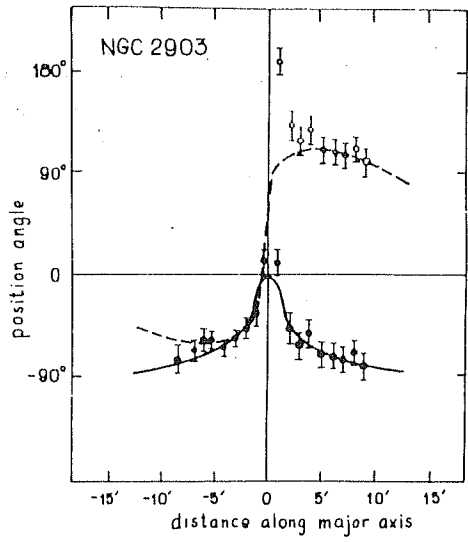


Fig. 8

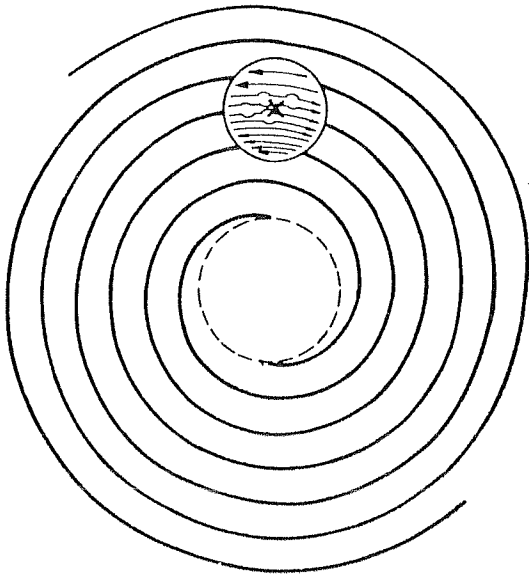


Fig. 9

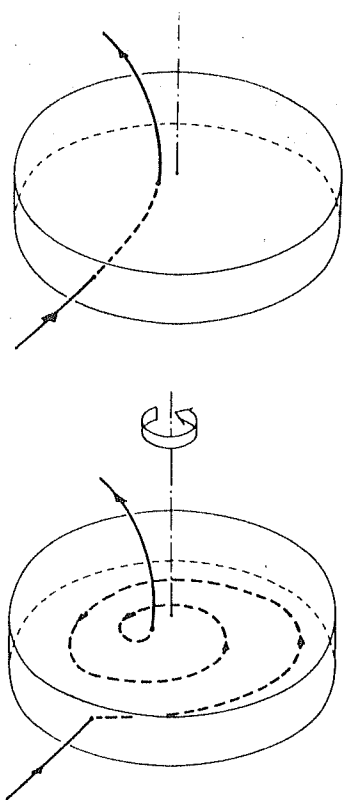


Fig. 10

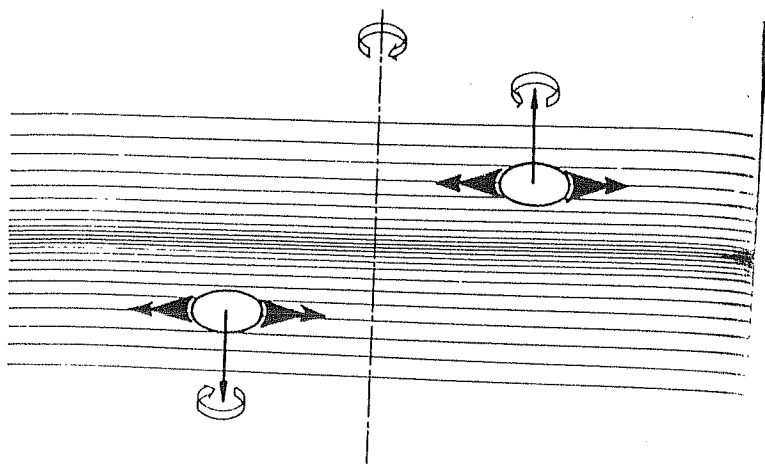


Fig. 11

CHAPTER II

AN INFINITELY THIN MAGNETIZED PLASMA DISK IN THE GRAVITATIONAL FIELD OF THE GALACTIC BULGE - A SELF-CONSISTENT TREATMENT

2.1. Introduction

As was described in the previous chapter, theories of galactic magnetic field suffer from several difficulties. We think that most of the difficulties stems from the fact that they are kinematical in nature and a complete dynamical treatment, we hope, shall remove the difficulties encountered by them. Therefore, it calls for a complete MHD analysis of the phenomena in the galactic disk.

We shall be considering the dynamics of a thin magnetized plasma disk with a central bulge in a self-consistent manner as an eigen-value problem in anticipation that the different magnetic field morphologies will turn out to be the normal mode of the system. The magnetic field morphologies should be the outcome of the dynamics of the system and that they should draw their energy from the gravitational field of the bulge. Rigid rotation is the only permissible solution of an equilibrium induction equation. As was noted in the previous chapter, differential rotation of the galactic disk and finite electrical resistivity of the ionized matter are the paramount condition for a galactic dynamo to function and we hope, dynamical treatment of the problem (i.e. coupling of magnetic force with the gravitational force through motion) will give us the different magnetic field morphologies as the normal modes of the systems.

We first study the magnetized plasma disk with a central bulge with the assumption that the fluid is incompressible. We derive an eigen-value equation for an incompressible plasma and see that fluid is unstable against gravity. Rayleigh-Taylor instability exists in the disk i.e. top-heavy arrangement is that of plasma density gradient supported by magnetic field against gravity. Ultimate source of energy turns out to be the gravitational energy which causes the growth of the magnetic field.

Next, in section 2.7, we consider a more general isothermal equation of state and recast the whole

eigen-value problem in the matrix form and solve numerically the general eigen-value problem. The eigenmodes are considered. Eigenmodes and eigenpatterns have been analyzed.

We discuss the basic magnetohydrodynamic equation in section 2.2. In section 2.3, we consider the equilibrium of the disk. In section 2.4., we describe the normal mode analysis. Section 2.5 discusses the instability and its growth rate. In section 2.6, we recast the eigenvalue equation in the variational form. In section 2.7, we discuss a more general equation of state and derive a density distribution consistent with the equilibrium of the system. Section 2.8 describes the non-dimensionalization of the different quantities. Section 2.9 discusses the Maxwell's equation and related with it the dispersion relation. In section 2.10 we discuss the general matrix formulation of the problem and finally, section 2.11 describes the numerical results.

2.2. Magnetohydrodynamic Equations

We study here the amplification of the magnetic field perturbation in an infinitesimally thin magnetized plasma disk with a central bulge. One knows that only a fraction of the galactic matter is in ionized form (~ 3 to 4%) and rest of it consists of neutral component. The ionized and the neutral components in the galactic disk interact via collisions which exchange momentum and energy between them.

It is assumed here that ion-neutral collision is negligible since their frictional time-scale is typically short (6×10^5 years, Spitzer, 1968) compared to the dynamical time-scale (10^6 years or more). Therefore, we consider a disk consisting of one fluid which represents the ionized component.

It is further assumed that the plasma in the disk is charge-neutral, since for a typical value of electrical conductivity $\sigma \sim 10^{-8} \text{ s}^{-1}$ and $\epsilon \sim 1$, time of charge separation $\sim 10^{-8} \text{ s}$. Because of the charge neutrality

$$\nabla \cdot \mathbf{j} = 0$$

i.e. currents must flow either in closed loops or in infinitely long circuits.

We must also assume that the plasma in the disk is infinitely conducting, i.e. $\sigma \rightarrow \infty$. Infinite conductivity ($\sigma \rightarrow \infty$) is a good approximation in most of the astrophysical situations. The gigantic scale-length involved in the heavenly processes ensures its validity. Magnetic Reynold number describes the relative importance of whether the magnetic fields are "frozen" in the matter or it diffuses with time. It is defined as

$$R_m = \sigma V \mu L$$

Where L is the characteristic scale-length, V -velocity of the fluid element, σ -the electrical conductivity of the fluid and μ -the magnetic permeability of the vacuum. Numerically, if σ is in s^{-1} , v in cm s^{-1} , and L in cm , we have

$$R_m \sim 1 \times 10^{20} \sigma L V$$

In cosmic plasmas, R_m nearly always turns out to be large compared to unity. For example, for solar convection zone $R_m \sim 10^8$; for an interstellar HI region $R_m \sim 10^3$; for HII region $R_m \sim 10^6$. On the other hand, in laboratory fluids we seldom have $R_m > 1$; for example, in a vat of mercury about 1m in size, we might have $R_m \sim 10^{-1}$.

Note that R_m is proportional to the product σL . Hence a large value of R_m resulting from enormous linear dimension (large L) is equivalent to a large value of electrical conductivity σ . Thus, cosmic plasma behave in much the same way as would a laboratory fluid with infinite conductivity.

[One] fluid Magnetohydrodynamic equations which describes the dynamics of a magnetized gravitating plasma disk, in the infinite conductivity limit are,

$$\rho \frac{d\mathbf{v}}{dt} = -\nabla p - \frac{GM}{r^2} \mathbf{r} + \mathbf{j} \times \mathbf{B} \quad (1)$$

$$\frac{\partial \rho}{\partial t} + \nabla \cdot (\rho \mathbf{v}) = 0 \quad (2)$$

$$\mathbf{E} + \mathbf{v} \times \mathbf{B} = 0 \quad (3)$$

$$\nabla \cdot \mathbf{v} = 0 \quad (4)$$

$$\nabla \times \mathbf{E} = - \frac{\partial \mathbf{B}}{\partial t} \quad (5)$$

$$\nabla \times \mathbf{B} = \mu \mathbf{j} \quad (6)$$

$$\underline{\nabla} \cdot \underline{B} = 0 \quad (7)$$

Equation (1) is the momentum balance equation, with ρ - the mass density and \underline{v} the mean or macroscopic plasma fluid velocity. The plasma is assumed electrically neutral and the particle pressure tensor is assumed to be a scalar. The time derivative here is the total derivative, taken moving along the fluid.

$$\frac{d}{dt} = \frac{\partial}{\partial t} + \underline{v} \cdot \underline{\nabla}$$

Equation (3) is Ohm's law in infinite conductivity limit. It shows that \underline{E} has no component parallel to \underline{B} . Secondly, \underline{v}_{\perp} , the part of \underline{v} is perpendicular to \underline{B} is given by $\underline{E} \times \underline{B}$ drift.

Equation (4) is the equation of state, which tells that fluid is incompressible. We assume this to be the case for the present treatment.

Equations (5), (6) and (7) are Maxwell's equation with the neglect of the displacement current.

By taking curl of equations (3) and making use of equation (5), we have the equation of induction in the infinite conductivity limit.

$$\frac{\partial \underline{B}}{\partial t} - \underline{\nabla} \times \underline{v} \times \underline{B} = 0 \quad (3')$$

Meaning of equation (3') will become more transparent, if one considers the change of magnetic flux Φ ,

$$\Phi = \int_S \underline{B} \cdot d\underline{S} \quad (8)$$

S is a surface that moves along with the fluid velocity and is bounded by a fixed contour c . Rate of change of flux of a vector field A through a moving surface S (Smyrnov, 1964), is given by

$$\frac{d}{dt} \int_S \underline{A} \cdot d\underline{S} = \int_S \left[\frac{\partial \underline{A}}{\partial t} + \underline{v} \cdot (\nabla \cdot \underline{A}) + \nabla \times (\underline{A} \times \underline{v}) \right] d\underline{S}$$

Hence,

$$\frac{d\Phi}{dt} = \int_S \left[\frac{\partial \underline{B}}{\partial t} - \nabla \times \underline{v} \times \underline{B} \right] \cdot d\underline{S} \quad (9)$$

Equation (9) states that for a perfectly conducting fluid the magnetic flux through any contour following the material motion remains constant in time. Alfven has described the consequence of (9) by saying that the magnetic lines of force are "frozen" into the fluid.

2.3. Equilibrium for a Flat Disk

Spiral galaxies are known to be highly flattened structures with a thickness of typically ~ 400 pc and a radius $R \sim 10$ kpc, so that $h/R \sim 0.04$. They can thus be modelled as infinitesimally thin discs to the lowest order.

A cylindracal system of coordinates (r, φ, z) is adopted. Since the disk is infinitesimally thin, all the physical quantities are restricted to $z=0$ plane, i.e.

$$\begin{aligned} \rho(r, \varphi, z, t) &= \sigma(r, \varphi, t) \delta(z) \\ \underline{J}(r, \varphi, z, t) &= \underline{J}(r, \varphi, t) \delta(z) \end{aligned}$$

$$P(r, \varphi, z, t) = p(r, \varphi, t) \delta(z)$$

where, $\sigma(r, \varphi, t)$, $j(r, \varphi, t)$ are the surface matter density and surface current density. p is pressure per unit length in the plane of the disk. Further,

$$\underline{v} = (v_r, v_\varphi, 0)$$

that, in a thin disk, material is confined to the (r, φ) -plane and hence $v_z \equiv 0$. Vorticity of the fluid is perpendicular to the plane of the disk. Therefore, both the r and φ components of $(\nabla \times \underline{v})$ vanish.

$$(\nabla \times \underline{v})_\varphi = 0$$

and,

$$(\nabla \times \underline{v})_r = 0$$

From where, one gets (since $v_z \equiv 0$)

$$\frac{\partial v_r}{\partial z} = 0$$

and,

$$\frac{\partial v_\varphi}{\partial z} = 0$$

Therefore,

$$\underline{v} = (v_r(r, \varphi, t), v_\varphi(r, \varphi, t), 0)$$

Momentum balance equation (1) can be written as:

$$\delta(z) \sigma \left[\frac{\partial \underline{v}}{\partial t} + (\underline{v} \cdot \nabla) \underline{v} \right] = -\nabla p \delta(z) - \sigma \delta(z) \frac{GM}{r^2} + \underline{J} \times \underline{B} \delta(z)$$

Which after integration over z gives:

$$\sigma \left[\frac{\partial \underline{v}}{\partial t} + (\underline{v} \cdot \nabla) \underline{v} \right] = -\nabla p - \frac{GM}{r^2} \sigma + \underline{j} \times \underline{B}$$

The continuity equation (2)

$$\frac{\partial \rho}{\partial t} + \nabla \cdot (\rho \underline{v}) = 0$$

likewise is

$$S(z) \frac{\partial \sigma}{\partial t} + \frac{1}{r} \left[\frac{\partial}{\partial r} (r \sigma v_r) + \frac{\partial}{\partial \varphi} (r \sigma v_\varphi) \right] S(z) = 0$$

So that, after integration over z , it becomes

$$\frac{\partial \sigma}{\partial t} + \frac{1}{r} \left[\frac{\partial}{\partial r} (r \sigma v_r) + \frac{\partial}{\partial \varphi} (r \sigma v_\varphi) \right] = 0$$

The induction equation is

$$\frac{\partial \underline{B}(r, \varphi, 0, t)}{\partial t} = \nabla \times \underline{v} \times \underline{B}$$

While the incompressibility condition (4) is:

$$\frac{\partial}{\partial r} (r v_r) + \frac{\partial v_\varphi}{\partial \varphi} = 0$$

Writing equilibrium induction equation in cylindrical (r, φ, z) coordinate

$$\frac{\partial}{\partial r} (B_{\varphi} v_0) + \frac{\partial}{\partial z} (v_0 B_{\varphi z}) = 0$$

why $B_{\varphi 0} = 0$?

and using $\nabla \cdot \underline{B} = 0$, i.e.

$$\frac{1}{r} \frac{\partial}{\partial r} (r B_{0r}) + \frac{\partial B_{0z}}{\partial z} = 0$$

Plugging it in the induction equation, one gets:

$$- \frac{B_{0r} V_0}{r} + B_{0r} \frac{dv_z}{dr} = 0$$

From where,

$$V_0 = r \Omega_0 \quad (10)$$

i.e. the only permissible consistent solution of Ohm's law is rigid rotation of the disk. Taking into account the rigid rotation of the disk and integrating the momentum balance equation over z , one gets the following equilibrium equation.

$$-\sigma_0 r \Omega_0^2 = - \frac{d\phi_0}{dr} - \frac{GM}{r^2} \sigma_0 + J_0 \varphi B_{0z}$$

It was seen in the last chapter that the dynamos cannot be sustained without differential rotation. On the other hand as noted above, differential rotation would require a non-zero electrical resistivity for an equilibrium solution. It would then appear that no dynamo equation of magnetic field would be possible with infinite conductivity which leads to a rigidly rotating disk. We shall, however, see that in the present self-consistent dynamical treatment of the problem the gravitational energy is converted into the

magnetic energy through the agency of the Rayleigh-Taylor instability, and the rigid rotation is no constraint. Magnetic perturbation grow even in the rigidly rotating equilibrium disk.

To know the equilibrium magnetic field, one solves the Maxwell's equation for the equilibrium current in the following way

$$\nabla \times \underline{B} = \underline{j}$$

Using $\underline{B} = \nabla \times \underline{A}$, one gets,

$$\nabla \times (\nabla \times \underline{A}) = \underline{j} \quad (6')$$

For azimuthal current,

$$[\nabla^2 \underline{A}]_{\varphi} = \int^{\infty} j_{\varphi}(r) \delta(z)$$

where j_{φ} is the equilibrium azimuthal current. Solution of the above Poisson equation is (Panofsky and Phillips, 1964).

$$A_{\varphi}(r, z) = \iint dk' dr' J_1(kr') J_1(kr) e^{-k|z|} j_{\varphi}(r') \quad (11)$$

With

$$B_{0r}(r, z) = - \frac{\partial}{\partial z} A_{\varphi}(r, z)$$

$$B_{0z}(r, z) = \frac{1}{r} \frac{\partial}{\partial r} (r A_{\varphi}(r, z))$$

We see that the radial component of the magnetic field changes sign across $z=0$ i.e. $B_{0r}(r, |z|=0) = 0$. On the other hand, $B_{0z}(r, z)$ remains continuous throughout. Source of

discontinuity of B_r is azimuthal current. This follows from integration of Maxwell's equation over z :

$$\int_{-\epsilon}^{+\epsilon} J_{0\varphi}(r) \delta(z) dz = \frac{\partial B_{0r}}{\partial z} - \frac{\partial B_{0z}}{\partial r}$$

Integrating over z from $z=-\epsilon$ to $z=+\epsilon$, then yields

$$2 B_r(r, \pm 0) = \int_{-\epsilon}^{+\epsilon} J_{0\varphi}(r) dz \quad (12)$$

Since

$$\lim_{\epsilon \rightarrow 0} \int_{-\epsilon}^{+\epsilon} B_{0z}(r, z) dz \approx \lim_{\epsilon \rightarrow 0} \left[B_z(r, z) \Delta z \right]_{-\epsilon}^{+\epsilon} = 0$$

Writing momentum balance equation with $\frac{\partial \varphi}{\partial \varphi} = 0$ and azimuthal current and rotational velocity $V_0 = r\Omega$:

$$-\sigma_0 r \Omega^2 = - \frac{dp_0}{dr} - \sigma_0 \frac{GM}{r^2} + \frac{2 B_{0r} B_{0z}}{r}$$

where the use has been made of (11). Equation of radial equilibrium, can be rewritten as:

$$\sigma_0 \left(\frac{GM}{r^2} - r \Omega^2 \right) = - \frac{dp_0}{dr} + \frac{2 B_{0r} B_{0z}}{r} \quad (13)$$

2.4. Normal Mode Analysis

As we have seen above, the equilibrium disc has an axisymmetric poloidal magnetic field supported by an azimuthal current density. This current density $J_{0\varphi}$ then

supports the imbalance between the pressure gradient, gravitational force and the inertial force. Such a disc could be Rayleigh-Taylor unstable to global perturbations if there exist inverted density gradients somewhere in the disc. A global mode of magnetic perturbation could thus grow at the expense of the gravitational energy of the system and could be identified with the observed global structure if it has an appropriate azimuthal symmetry. To this end we study the stability of the disc.

We study the stability of this thin magnetized plasma disk by using normal mode analysis.

Now, consider a non-axisymmetric perturbation in the density, pressure, current and velocity over its equilibrium values in the disk. Perturbation in current in turn causes a perturbation in the magnetic field. We assume all the perturbed quantities to be small compared to the corresponding equilibrium quantities, so that a linearization around unperturbed quantities can be carried out. Thus we write the net quantities as

$$\begin{aligned}
 \sigma(r, \varphi, t) &= \sigma_0(r) + \epsilon \tilde{\sigma}(r, \varphi, t) \\
 P(r, \varphi, t) &= P_0(r) + \epsilon \tilde{P}(r, \varphi, t) \\
 \underline{v}(r, \varphi, t) &= \underline{v}_0(r) + \epsilon \tilde{\underline{v}}(r, \varphi, t) \\
 \underline{j}(r, \varphi, t) &= \underline{j}_0(r) + \epsilon \tilde{\underline{j}}(r, \varphi, t) \\
 \underline{B}(r, \varphi, z, t) &= \underline{B}_0(r, z) + \epsilon \tilde{\underline{B}}(r, \varphi, z, t)
 \end{aligned}
 \tag{14}$$

Where,

$$\tilde{\underline{j}}(r, \varphi, t) = (\tilde{j}_r, \tilde{j}_\varphi, 0)$$

$$\underline{v}(r, \varphi, t) = (\tilde{v}_r, \tilde{v}_\varphi, 0)$$

where σ , p , \underline{v} , \underline{j} and \underline{B} represents the surface density, pressure, velocity, surface current density and magnetic field respectively. We recall that the velocity in equilibrium is entirely azimuthal, and corresponding to a rigid rotation,

Substituting (14) in equation (1)-(6) and linearizing and integrating over z , we get the following equations for the perturbed quantities:

$$\left. \begin{aligned} \sigma_0 \left[\left(\frac{\partial}{\partial t} + \Omega_0 \frac{\partial}{\partial \varphi} \right) \tilde{v}_r - 2\Omega_0 \tilde{v}_\varphi \right] - r\Omega_0^2 \tilde{r} &= - \frac{d\tilde{p}}{dr} - \left\{ \right. \\ &\quad \left. - \tilde{\sigma} \frac{GM}{r^2} + \frac{2B_{0r} \tilde{b}_z}{r} + \frac{2\tilde{b}_r B_{0z}}{r} \right\} \\ \sigma_0 \left[\left(\frac{\partial}{\partial t} + \Omega_0 \frac{\partial}{\partial \varphi} \right) \tilde{v}_\varphi + 2\Omega_0 \tilde{v}_r \right] &= - \frac{1}{r} \frac{\partial \tilde{p}}{\partial \varphi} + \frac{2\tilde{b}_\varphi B_{0z}}{r} \end{aligned} \right\} \quad (15)$$

Induction equation (3) becomes

$$\left. \begin{aligned} \left(\frac{\partial}{\partial t} + \Omega_0 \frac{\partial}{\partial \varphi} \right) \tilde{b}_r &= \tilde{v}_r \left(\frac{\partial B_{0z}}{\partial z} \right)_{z=0} - \frac{B_{0r}}{r} \frac{\partial \tilde{v}_\varphi}{\partial \varphi} \\ \left(\frac{\partial}{\partial t} + \Omega_0 \frac{\partial}{\partial \varphi} \right) \tilde{b}_\varphi &= \tilde{v}_\varphi \left[\left(\frac{\partial B_{0z}}{\partial z} \right)_{z=0} \right] + \frac{\partial}{\partial r} (\tilde{v}_r B_{0z})_{z=0} \\ \left(\frac{\partial}{\partial t} + \Omega_0 \frac{\partial}{\partial \varphi} \right) \tilde{b}_z &= - \frac{1}{r} \left[\frac{\partial}{\partial r} (r \tilde{v}_r B_{0z}) + \frac{\partial}{\partial \varphi} (\tilde{v}_\varphi B_{0z}) \right]_{z=0} \end{aligned} \right\} \quad (16)$$

where use has been made of the fact

$$\tilde{j}_\varphi(r) = 2r^n \tilde{b}_r(r, 0)$$

$$\tilde{J}_r(r) = -2\gamma^n \tilde{b}_\varphi(r, 0)$$

where tilda denotes the perturbed quantities whereas index 0 means equilibrium quantities.

The above set of partial differential equations (15-16) involves terms with coefficients which are constant with respect to φ and t but depend on r explicitly. We can then Fourier analyze with respect to the azimuthal angle φ and time t , and thus seek a solution in the form:

$$\tilde{A}(r, \varphi, t) = \hat{A}(r) \exp [i(\omega t - m\varphi)] \quad (17)$$

Where \tilde{A} stands for any perturbed quantity. The resulting set of equations can be reduced to one ordinary differential equation in terms of radial velocity \tilde{v}_r , which must be solved as an eigen value problem with appropriate boundary conditions.

In equation (17) ω is the frequency of the perturbation and in general, is complex; m is the azimuthal wave number. The frequency $\omega = \omega_r + i\omega_i$ such that the pattern-velocity $\Omega_p = \omega_r/m$ and ω_i represents the temporal growth rate of the perturbation. Using equation (17) along with $\frac{1}{r} \frac{\partial}{\partial r} (r \tilde{v}_r) = \frac{im}{r} \tilde{v}_\varphi$, set of equations (15-16) can be written in the following form:

Continuity

$$\lambda (\omega - m\Omega_0) \tilde{\sigma} + \tilde{v}_r \frac{d\sigma_0}{dr} = 0$$

Equations of motion:

$$\begin{aligned} \sigma_0 \left[i(\omega - m\Omega_0) \tilde{v}_r - 2\Omega_0 \tilde{v}_\varphi \right] + \delta \left(\frac{GM}{r^2} - r\Omega_0^2 \right) &= \\ &= - \frac{d\tilde{p}}{dr} + \frac{2B_{0r} \tilde{b}_z}{r} + \frac{2\tilde{b}_r B_{0z}}{r} \\ \sigma_0 \left[i(\omega - m\Omega_0) \tilde{v}_\varphi + 2\Omega_0 \tilde{v}_r \right] &= \frac{im}{r} \tilde{p} + \frac{2\tilde{b}_\varphi B_{0z}}{r} \end{aligned}$$

Induction equations:

$$\left. \begin{aligned} \lambda (\omega - m\Omega_0) \tilde{b}_r &= - \frac{\tilde{v}_r}{r} \frac{d}{dr} (r B_{0r}) + \frac{im}{r} \tilde{v}_\varphi B_{0r} \\ \lambda (\omega - m\Omega_0) \tilde{b}_\varphi &= r B_{0r} \frac{d}{dr} \left(\frac{\tilde{v}_\varphi}{r} \right) \\ \lambda (\omega - m\Omega_0) \tilde{b}_z &= - \tilde{v}_r \frac{dB_{0z}}{dr} \end{aligned} \right\} \quad (18)$$

Pressure p is eliminated between the r and φ component of the momentum balance equation. Also using the induction equation (18) to eliminate \tilde{b}_r , \tilde{b}_φ and \tilde{b}_z we get the following differential equation for ,

$$\begin{aligned} \frac{d^2}{dr^2} (r \tilde{v}_r) \left[(\omega - m\Omega_0)^2 + \frac{2B_{0r}}{r\sigma_0} \frac{dB_{0z}}{dr} \right] + \\ + \frac{1}{r} \frac{d}{dr} (r \tilde{v}_r) \left[(\omega - m\Omega_0)^2 \left(\frac{r}{\sigma_0} \frac{d\sigma_0}{dr} + 1 \right) - \frac{2B_{0r}}{r\sigma_0} \frac{dB_{0z}}{dr} \right] = \end{aligned}$$

$$-\left(\frac{m}{r}\right)^2 (r \tilde{v}_r) \left[(\omega - m \Omega_0)^2 - \frac{2(\omega - m \Omega_0) r \Omega_0 d\sigma_0}{m \sigma_0} \frac{d\sigma_0}{dr} + \right. \\ \left. + \frac{1}{\sigma_0} \frac{d\sigma_0}{dr} \left(\frac{GM}{r^2} - r \Omega_0^2 \right) - \frac{2 B_{0r}}{\mu \sigma_0} \frac{dB_{0z}}{dr} \right] = 0 \quad (19)$$

2.5. Discussion

If for simplicity, one takes $r \tilde{v}_r = \text{constant}$ and $\frac{1}{\sigma_0} \frac{d\sigma_0}{dr} \ll 1$, then one gets

$$(\omega - m \Omega_0)^2 = - \frac{1}{\sigma_0} \frac{d\sigma_0}{dr} \left(\frac{GM}{r^2} - r \Omega_0^2 \right) + \frac{2 B_{0r}}{\mu \sigma_0} \frac{dB_{0z}}{dr} \quad (20)$$

which can be rewritten in terms of pressure gradient and magnetic field equation (13)

$$(\omega - m \Omega_0)^2 = \frac{1}{\sigma_0^2} \frac{d\sigma_0}{dr} \frac{dp_0}{dr} + \frac{2 B_{0r}}{\sigma_0 \mu} \frac{d}{dr} \left(\frac{B_{0z}}{\sigma_0} \right) \quad (21)$$

Relation (20) determines the stability of the system. Writing $\omega = \omega_r + i \omega_i$, the time dependence of the solution is

$$\text{Exp} [i(\omega_r t + i \omega_i t)] = \text{Exp} [i \omega_r t] \cdot \text{Exp} [-\omega_i t]$$

and hence perturbation grows and mode is unstable if $\omega_i < 0$. From (20), it is clear that, for instability

$$\frac{2 B_{0r}}{\mu \sigma_0} \frac{d}{dr} (B_{0z}) < \frac{1}{\sigma_0} \frac{d\sigma_0}{dr} \left(\frac{GM}{r^2} - r \Omega_0^2 \right)$$

or, from equation (21)

$$\frac{2 B_{0r}}{r^n} \frac{d}{dr} \left(\frac{B_{0z}}{\sigma_0} \right) < - \frac{1}{\sigma_0^2} \frac{d\sigma_0}{dr} \frac{dp_0}{dr}$$

Therefore, growth rate is given by

$$\left[- \frac{1}{\sigma_0} \frac{d\sigma_0}{dr} \left(\frac{GM}{r^2} - r \Omega_0^2 \right) + \frac{2 B_{0r}}{r^n} \frac{dB_{0z}}{dr} \right]^{\frac{1}{2}}$$

From the above expression, we see that the instability grows faster for large positive density gradient. First term in the expression for the growth rate is density gradient times the imbalance of gravitational and centrifugal forces. As the matter spirals towards the bulge, amount of energy released is proportional to the imbalance of gravitational and centrifugal terms. This energy is converted into magnetic energy by twisting of the field lines by the infalling rotating matter.

Expressing through pressure gradient and magnetic force, from the equilibrium equation, the imbalance of gravitational and centrifugal force, one gets the growth rate as

$$\left[\frac{1}{\sigma_0^2} \frac{d\sigma_0}{dr} \frac{dp_0}{dr} + \frac{2 B_{0r}}{r^n} \frac{d}{dr} \left(\frac{B_{0z}}{\sigma_0} \right) \right]^{\frac{1}{2}}$$

i.e. instability grows faster for the steeper pressure gradient. Assuming $P = C_s^2 \sigma_0$ and taking $C_s^2 = 57 \times 10^3 \text{ cm}^2/\text{s}^2$ and $C_s^2 = 11 \times 10^5 \text{ cm}^2/\text{s}^2$ for HI and HII region respectively (Spitzer, 1968) and corresponding spread of this region to

be $L_{HI} \sim 3 \times 10^{19}$ cm and $L_{HII} \sim 3 \times 10^{20}$ cm, one gets the growth rate

$$\left[\text{Im}(\omega - m\Omega_0) \right]_{HI \text{ region}} \approx \frac{c_s}{R} \approx 6 \times 10^{-9} \text{ yr}^{-1}$$

Therefore, for over the galactic life time $\sim 10^{10}$ Yr field amplification is $\sim \text{Exp}^{60}$. For $t_{\text{galaxy}} \sim 10^8$ Yr field amplification is $\sim \text{Exp}^{0.6}$ times only.

$$\left[\text{Im}(\omega_0 - m\Omega_0) \right]_{HII \text{ region}} \approx 10^{-8} \text{ yr}^{-1}$$

Over the galactic life time field gets amplified Exp^{100} times. In the case of high red-shift ($Z=4$) when age of the galaxy was $\sim 10^8$ Yr, field amplification $\sim \text{Exp}^{(1-2)}$.

A simplification can be affected in equation (19) by invoking a WKBJ approximation and writing

$$\tilde{A}(r) = \hat{A}_0(r) \text{Exp} \left[i \int k(r') dr' \right] \quad (22)$$

Where $\hat{A}_0(r)$ is a very slowly varying function, whereas the exponential (phase) part is a rapidly varying function of r , that is, $kr \gg 1$.

Assuming $S = \gamma \tilde{v}_r$ and expressing S as in (22), we can write the dispersion relation, after simple algebraic manipulation, in the following form:

$$(\omega - m\Omega)^2 \left[k^2 - ik \left(\gamma \frac{d}{dr} \ln \sigma_0 \right) \right] + k^2 \frac{2B_{0r}}{\mu \sigma_0} \frac{dB_{0z}}{dr} = 0$$

From where

$$(\omega - m\Omega_0)^2 = \left(\frac{2B_{0r}}{\mu\sigma_0} \frac{dB_{0z}}{dr} \right) \frac{k}{k\sigma_0 - i \frac{d\sigma_0}{dr}}$$

and from equilibrium

$$\begin{aligned} \frac{2B_{0r}}{\mu} \frac{dB_{0z}}{dr} &= \frac{GM}{r^2} \left(\frac{r}{\sigma_0} \frac{d\sigma_0}{dr} - 2 \right) + \\ &+ r\Omega_0^2 \left(\frac{r}{\sigma_0} \frac{d\sigma_0}{dr} - 1 \right) + \frac{r}{\sigma_0} \frac{d^2 p_0}{dr^2} + \\ &+ \frac{2rB_{0z}}{\mu} \frac{dB_{0r}}{dr} \end{aligned}$$

Therefore,

$$(\omega - m\Omega_0)^2 = - \left\{ \frac{k}{k\sigma_0 - i \frac{d\sigma_0}{dr}} \right\} \left(\frac{GM}{r^2} - \frac{r}{\sigma_0} \frac{d^2 p_0}{dr^2} - \frac{2rB_{0z}}{\mu} \frac{dB_{0z}}{dr} \right)$$

Growth rate is given by

$$\left[\left\{ \frac{k}{k\sigma_0 - i \frac{d\sigma_0}{dr}} \right\} \left(\frac{GM}{r^2} - \frac{r}{\sigma_0} \frac{d^2 p_0}{dr^2} - \frac{rB_{0z}}{\mu} \frac{dB_{0z}}{dr} \right) \right]^{1/2}$$

We see that as $k \rightarrow \infty$, $\omega \rightarrow \infty$, for the short wavelength, instability grows very fast. Magnetic field growth is caused by the infalling matter towards the center.

The above study indicates that the density gradient of

the ionized gas in the disk and the pressure gradient causes the growth of the magnetic field in the disk. Field draws its energy from the "density and pressure gradients" of the gas. Steeper the change in density of the gas, faster the instability grows. This instability should have been anticipated on the ground that in the galactic disk, the arrangement is "top-heavy" of a magnetized plasma against a gravitational field.

2.6. Variational Technique

We now come to a technique that is often used in stability analysis. The technique is to construct a variational form of the eigen-equation (19) since it is difficult to construct even an approximate solution for it as an eigenvalue problem. We need to use a generalized variational technique, associated with the eigenenergy of a system to the eigenvalue equation. Following Moisewitch (variational principles), we should construct our eigen equation in the form:

$$L S = \lambda M S \quad (23)$$

where L and M denotes differential operators. Introducing adjoint operators

$$\tilde{L} \bar{S} = \lambda \tilde{M} \bar{S} \quad (24)$$

where the adjoint operators \tilde{L} and \tilde{M} together with the adjoint solution \bar{S} is defined in such a way that the

relations

$$\int \bar{\delta} L S d\tau = \int S \tilde{L} \bar{S} d\tau, \quad \int \bar{S} M S d\tau = \int S \tilde{M} \bar{S} d\tau \quad (25)$$

are satisfied, the integration being performed over the volume.

Multiplying both sides of (23) by \bar{S} and integrating over yields

$$\lambda = I[S] \quad (26)$$

where,

$$I[S] = \frac{\int \bar{S} L S d\tau}{\int \bar{S} M S d\tau} \quad (27)$$

The change in $I[S]$ due to infinitesimal variation δS and $\delta \bar{S}$ in S and \bar{S} respectively is

$$\begin{aligned} \delta I[S] \int \bar{S} M S d\tau + I[S] \int \delta \bar{S} M S d\tau + I[S] \int \bar{S} M \delta S d\tau &= \\ &= \int \delta \bar{S} L S d\tau + \int \bar{S} L \delta S d\tau \end{aligned}$$

neglecting $O(\delta^2)$ quantities. Provided δS and $\delta \bar{S}$ satisfies appropriate boundary conditions, one can put

$$\int \bar{S} L \delta S d\tau = \int \delta S \tilde{L} \bar{S} d\tau$$

and

$$\int \bar{S} M \delta S d\tau = \int \delta S \tilde{M} \bar{S} d\tau$$

and therefore

$$\delta I[S] = \frac{\int \delta \bar{S} (L S - \lambda M S) d\tau + \int \delta S (\tilde{L} \bar{S} - \lambda \tilde{M} \bar{S}) d\tau}{\int \bar{S} M S d\tau}$$

We know that S and S are solutions of (23) and (24) respectively,

$$\int I[S] = 0$$

From the above description of the variational principle, it's clear that we need to reformulate our eigen-equation (19) in the form

$$LS = \lambda MS$$

Let us denote

$$S = r \tilde{v}_r, \quad \lambda = (\omega - m\Omega)^2$$

and $R = \frac{2 B_r}{r \sigma_0} \frac{dB_z}{dr}$, then (19) becomes

$$\begin{aligned} & \frac{d^2 S}{dr^2} \left[\lambda + R(r) \right] + \frac{1}{r} \frac{dS}{dr} \left[\lambda \left(\frac{r}{\sigma_0} \frac{d\sigma_0}{dr} + 1 \right) - R \right] - \\ & - \left(\frac{m}{r} \right)^2 S \left[\lambda - \frac{2\Omega\sqrt{\lambda}}{m} \frac{r}{\sigma_0} \frac{d\sigma_0}{dr} + \frac{1}{\sigma_0^2} \frac{d\sigma_0}{dr} \left(- \frac{dp_0}{dr} + \frac{2B_r B_{\theta 2}}{r} \right) - \right. \\ & \quad \left. - R(r) \right] = 0 \end{aligned}$$

Denoting by,

$$L = \frac{d^2}{dr^2} - \frac{1}{r} \frac{d}{dr} - \left(\frac{m}{r} \right)^2 \left[\frac{1}{R \sigma_0^2} \frac{d\sigma_0}{dr} \left(- \frac{dp_0}{dr} + \frac{2B_r B_{\theta 2}}{r} \right) - 1 \right]$$

and assuming $\frac{r}{\sigma_0} \frac{d\sigma_0}{dr} \ll 1$, we can rewrite the eigen-equation

in the form (23). Differential operators L and M are not self-adjoint and hence equation (24) can not be satisfied.

To make L self-adjoint, one multiplies L by $1/r$. Therefore, $\tilde{L} = L/r$. But M/r is not self-adjoint operator, and to make it self-adjoint, one assumes that

$$R(r) := \frac{2 B_0 r}{m \epsilon_0} \frac{dB_z}{dr} = \frac{1}{r^2}$$

Then,

$$\tilde{M} = - \left[-r \frac{d^2}{dr^2} + \frac{d}{dr} - r \left(\frac{m}{r} \right)^2 \right]$$

and, therefore:

$$\tilde{L} \tilde{S} = \lambda \tilde{M} \tilde{S}$$

Equation (25) is automatically satisfied. In our problem, which possesses cylindrical symmetry, (25) can be rewritten as

$$\int \tilde{S} L S r dr = \int \tilde{S} \tilde{L} \tilde{S} r dr$$

and,

$$\int \tilde{S} M S r dr = \int S \tilde{M} \tilde{S} r dr$$

and,

$$\lambda = I[S], \quad I[S] = \frac{\int \tilde{S} L S r dr}{\int \tilde{S} M S r dr}$$

We have to guess a function $S = f(r, \alpha)$ and from extremum of the functional $I[\alpha]$, i.e. $\frac{\partial I}{\partial \alpha} = 0$ one should find α 's. For $m=0$, we have constructed such a solution

$$\tilde{V}_r = -r \ln r$$

Plugging this solution in (25), one gets an upper bound on λ i.e. on $(\omega - \omega_0)^2$

$$\lambda \leq -2.31$$

or

$$\omega^2 \leq -4.34 \times 10^{-9} \gamma \gamma^{-1}$$

For axisymmetric mode, a solution of the eigen-equation goes to zero at the origin and at the boundary of the disk (Fig 2.1). An upper bound to the eigenenergy gives the minimum growth rate of the axisymmetric mode.

2.7. A More General Treatment

We study the equilibrium of a thin disk, as described in section 2.3, with a more general equation of state. We have assumed a polytropic equation of the form

$$P = C \rho^\gamma \quad (28)$$

Where, C and γ are constants. The acoustics velocity in the disk is given by

$$c_s^2 = \frac{dP}{d\rho} = C \gamma \rho^{\gamma-1}$$

The parameter C represents the measure of the randomness or "hotness" of the gas and γ is the polytropic index for

two-dimensional systems. Equation (28) can be related to an ordinary polytropic relation for the three dimensional medium of the form:

$$\Pi = K \rho^\alpha$$

Where Π and ρ are pressure and volume density respectively and K and α are constants. Hunter (1972) has obtained the relation

$$\gamma = 3 - \frac{2}{\alpha}, \quad C = \frac{\pi^{3/2 - 1/\alpha}}{2^{2 - 1/\alpha}} \cdot \frac{\Gamma(2 - 1/\alpha)}{\Gamma(5/2 - 1/\alpha)} K^{1/\alpha} \quad (29)$$

by taking a limit case of an infinitely thin disk. Here

Γ is a gamma function. Thus, the case with $r=1$ and $r=3$ in equation (28) corresponds to the equation of state (29) with $\alpha = 1$ (isothermal) and $\alpha = \infty$ (incompressible), respectively. From equation of state (28) assuming

$\gamma = 1$ (isothermal case), we can rewrite above equation as:

$$\frac{d\sigma_0}{d\gamma} + \sigma_0 \left(\frac{GM}{c_s^2 r^2} - \frac{r \Omega_0^2}{c_s^2} \right) = \frac{2 B_{01} B_{02}}{n c_s^2} \quad (13')$$

Solving above equation, one gets the self-consistent expression for the surface density in the disk:

$$\sigma_0(r) = \frac{1}{2\pi c_s^2} \exp\left(\frac{GM}{c_s^2 r} + \frac{(\Omega_0 r)^2}{2c_s^2}\right) \int_0^r e^{-\frac{(\Omega_0 \xi)^2}{2c_s^2} - \frac{GM}{c_s^2 \xi}} \times B_{01} B_{02} d\xi \quad (30)$$

Equation (30) can be employed to construct some models with special current density distribution in finite as well as infinite disks. We have considered one such model in equilibrium, before studying their stability against various perturbation.

For regular current distributions, such as

$$J_{0\varphi}(r) = \begin{cases} J_0\left(\frac{r}{R}\right) \left(1 - \frac{r^2}{R^2}\right) & r \leq R_{\text{disk}} \\ 0 & r > R_{\text{disk}} \end{cases}$$

z-component of the magnetic field is found to change sign along the disk. The circumstance is not occasional: it may be shown (Freedman and Polyachenko, 1984) that, at any regular current distribution, the field B_{0z} necessarily changes sign at $r \leq R_d$. This fact happens to be important in the analysis of the stability of such systems. It is very easy to prove that for any regular current, B_{0z} changes sign. We use for $J_{0\varphi}$ and B_{0z} somewhat different representations:

$$J_{0\varphi} = \frac{1}{\pi} \sqrt{1-\eta^2} \sum_{n=1}^{\infty} \frac{g_{2n} P'_{2n}(\eta)}{\gamma'_{2n}}$$

$$B_{0z} = \frac{1}{\pi} \sum_{n=1}^{\infty} g_{2n} P_{2n}(\eta)$$

where,

$$\gamma'_{2n} \equiv n(2n-1) \left[\frac{(2n-1)!!}{(2n)!!} \right]^2$$

$\eta = \sqrt{1 - \frac{r^2}{R_{disk}^2}}$; $P_{2n}'(\eta)$ is the derivative of the Legendre polynomial. In the expression for current and magnetic field, $n=0$ term is not considered, since it would correspond to singular term. This can be proved by rule of contraries, i.e. assume that B_{oz} does not change sign on the disk, say $B_{oz} > 0$. Then integrating B_{oz} from 0 to 1 over $d\eta$

$$\begin{aligned} 0 < \int_0^1 B_{oz} d\eta &= \frac{1}{r^n} \sum g_{2n} \int_0^1 P_{2n} d\eta = - \sum g_{2n} \left[\frac{\sum (1-\eta^2) P_{2n}'(\eta)}{2n(2n+1)} \right]_0^1 \\ &= - \sum_{n=1}^{\infty} \frac{g_{2n} (1-\eta^2) P_{2n}'(\eta)}{2n(2n+1)} \Big|_0^1 = 0 \end{aligned}$$

Thus, the component B_{oz} of a self-consistent magnetic field ought to change sign on the disk.

It is clear from equation (30) that integrand

$$B_{\phi} B_{oz} e^{-\left(\frac{\Omega_c^2 \xi^2}{2 \omega^4} + \frac{GM}{c^4 \xi} \right)}$$

will change sign along the disk making the density unphysical. Therefore regular current distribution can not be taken as equilibrium current and we take the current distribution of the following form (like Yobushita's, 1969 density distribution)

$$J_{\phi}(r) = \begin{cases} J_0 \sum_{j=0}^{\infty} a_j J_1(k_j r) & ; r \leq R_{disk} \\ 0 & ; r > R_{disk} \end{cases}$$

Where k_j 's are zero's of the transcendental equation

$$J_1(k_j R_{disk}) = 0$$

to ensure that the surface current density vanishes at the boundary of the disk.

We consider a particular current, with $j=1$ and $a_j=1$. $k = 3.83171$ is the first zero of the Bessel function. Plugging $j_0 \varphi(r) = I_0 J_1(k_0 r)$ in the expression (11), one gets the vector potential

$$A_0 \varphi(r, z) = \left(\frac{\mu_0 I_0}{2 k_0} J_1(k_0 r) e^{-k_0 |z|} \right)$$

From where,

$$B_{0r} \big|_{z=0} = \left(\frac{\mu_0 I_0}{2} J_1(k_0 r) \right)$$

and,

$$B_{0z} \big|_{z=0} = \left(\frac{\mu_0 I_0}{2} J_0(k_0 r) \right)$$

From above expression for B_{0r} and B_{0z} we see that integrand $B_{0r} B_{0z} \exp - \left(\frac{\Omega_0^2 \xi^2}{2 c^2} - \frac{GM}{c^2 \xi} \right)$ is positive definite throughout the disk i.e.:

$$\int B_{0r} B_{0z} \exp \left[\frac{\Omega_0^2 \xi^2}{2 c^2} - \frac{GM}{c^2 \xi} \right] d\xi \geq 0$$

The formalism for the above current density distribution, may be extended to other current distribution. We have not taken any other current distribution since the computational time required even with this model is large.

2.8. Non-Dimensional Equation

Non-dimensional function $\hat{\sigma}(\xi)$, $\hat{p}(\xi)$, $\hat{f}(\xi)$, $B(\xi)$ and $V(\xi)$ are introduced corresponding to the surface density, pressure

current density, magnetic field and velocity as follows:

$$\left. \begin{aligned} \sigma(r) &= \left(\frac{M}{2\pi R^2} \right) \hat{\sigma}(\xi) \\ \rho(r) &= \left(\frac{GM^2}{2R^3} \right) \hat{\rho}(\xi) \\ J(r) &= \frac{M}{R^2} \left(\frac{G}{2\pi} \right)^{1/2} \hat{J}(\xi) \\ B(r) &= \frac{M}{R^2} \left(2\pi G \right)^{1/2} \hat{B}(\xi) \end{aligned} \right\} \quad (31)$$

and

$$V(r) = \left(\frac{11 GM}{R} \right)^{1/2} \hat{V}(\xi)$$

where $\xi = \frac{r}{R_d}$, R_d is the radius of the disk and M -mass of the gravitational bulge. The angular velocity is measured in non-dimensional unit of time

$$\tau = \left(\frac{11 GM}{R^3} \right) t \quad (32)$$

Substituting equation (29)-(30) in (1)-(2) and dropping the cap from $\hat{\sigma}$, $\hat{\rho}$ etc. and writing r for ξ , t for τ , one obtains non-dimensionalized equation

$$J_{0\varphi}(r) = J_1(k_0 r)$$

$$B_{0r}(r) = \frac{J_1(k_0 r)}{2}$$

$$B_{0z}(r) = \frac{J_0(k_0 r)}{2}$$

and

$$\sigma_0(r) = \frac{1}{2} \exp\left(\frac{r^2}{2} + \frac{1}{r}\right) \int_0^r J_1(k_0 \xi) J_0(k_0 \xi) e^{-\left(\frac{\xi^2}{2} + \frac{1}{\xi}\right)} d\xi$$

The above density distribution for $\hat{\Omega}_0 = 1$, $K_0 = 3.8 \gg 1$, has been plotted in Fig. 2.2. Using (31) and (32) in equation (13), the non-dimensional radial equilibrium equation of motion becomes:

$$-\frac{V_0^2}{\gamma} = -\frac{1}{\sigma_0} \frac{d\sigma_0}{dr} - \frac{1}{r^2} + \frac{2 B_{0r} B_{0z}}{\sigma_0}$$

The central bulge has been assumed here to be spherical and contribute a term r^{-2} , at the plane of the disk in the above equation.

2.9. Solution of Maxwell's Equation and Dispersion Relation

Maxwell's equation (6') can be rewritten in the following form:

$$\left. \begin{aligned} \frac{1}{\gamma} \frac{\partial}{\partial r} \left(\gamma \frac{\partial F}{\partial r} \right) - \left(\frac{m-1}{\gamma} \right)^2 F + \frac{\partial^2 F}{\partial z^2} &= - (J_r + i J_\varphi) \hat{\delta}(z) \\ \frac{1}{\gamma} \frac{\partial}{\partial r} \left(\gamma \frac{\partial Q}{\partial r} \right) - \left(\frac{m+1}{\gamma} \right)^2 Q + \frac{\partial^2 Q}{\partial z^2} &= - (J_r - i J_\varphi) \hat{\delta}(z) \end{aligned} \right\} \quad (33)$$

where,

$$F = A_r + i A_\varphi$$

$$Q = A_r - i A_\varphi$$

(34)

and without loss of generality, one can assume $A_z = 0$ i.e.

$$\nabla^2 A_z = 0$$

Integrating equation (33) over z , one gets the "jump" condition:

$$\begin{aligned}\frac{\partial F}{\partial z} \Big|_{|z|=0} &= 2 (b_\varphi - i b_r) \\ \frac{\partial Q}{\partial z} \Big|_{|z|=0} &= 2 (b_\varphi + i b_r)\end{aligned}\quad (35)$$

where use has been made of the fact that radial and azimuthal component of the magnetic field suffers a discontinuity caused by the azimuthal and radial current respectively.

Solutions of equations (33), in the disk ($r < 1$) can be written as

$$\begin{aligned}F(r, z) &= \sum_{k=0}^{\infty} E_m J_{m-1}(kr) e^{-k|z|} \\ Q(r, z) &= \sum_{k=0}^{\infty} D_m J_{m+1}(kr) e^{-k|z|}\end{aligned}$$

Outside the disk ($r > 1$), equation (33) becomes Laplace's equation and their solution can be written as

$$\begin{aligned}F(r, z) &= \sum B_m N_{m-1}(kr) e^{-k|z|} \\ Q(r, z) &= \sum B_m N_{m+1}(kr) e^{-k|z|}\end{aligned}$$

Plugging the disk solution for $F(r, z)$ and $Q(r, z)$ in (35), multiplying both sides of the 1st and 2nd equation by $J_{m-1}(k'r)$ and $J_{m+1}(k'r)$ respectively and integrating over

rd r from 0 to 1, one gets:

$$E_m(k) = -\frac{2}{M} \int_0^1 (b_\varphi - i b_r) J_{m-1}(kr) r dr$$

and

$$D_m(k) = -\frac{2}{M_1} \int_0^1 (b_\varphi + i b_r) J_{m+1}(kr) r dr$$

Where

$$M = \frac{1}{2} [J_m(k)]^2 \quad ; \quad M_1 = \frac{1}{2} [J_{m+2}(k)]^2$$

From (34), one gets

$$A_r = \frac{F + Q}{2} \quad , \quad A_\varphi = \frac{F - Q}{2}$$

and therefore, one can write the solutions of Poisson's equation (33) in terms of vector potential in the disk as follows:

$$A_r = \frac{1}{2} \sum_{k=0}^{\infty} [D_m J_{m+1}(kr) + E_m J_{m-1}(kr)] e^{-k|z|}$$

$$A_\varphi = \frac{i}{2} \sum_{k=0}^{\infty} [D_m J_{m+1}(kr) - E_m J_{m-1}(kr)] e^{-k|z|}$$

outside the disk ($r > 1$)

$$A_r = \frac{e^{-k|z|}}{2} \sum_{k=0}^{\infty} B_m [N_{m+1}(kr) + N_{m-1}(kr)] \equiv \frac{m}{\gamma} \sum_{k=0}^{\infty} B_m \frac{N_m(kr) - k|z|}{k} e^{-k|z|}$$

$$A_\varphi = \frac{i e^{-k|z|}}{2} \sum_{k=0}^{\infty} B_m [N_{m+1}(kr) - N_{m-1}(kr)]$$

From the above expressions, magnetic fields inside and outside the disk are for $r < 1$

$$b_r = \frac{i}{2} \sum_{k=0}^{\infty} k [D_m J_{m+1}(kr) - E_m J_{m-1}(kr)]$$

$$b_{\varphi}|_{|z|=0} = -\frac{1}{2} \sum_{k=0}^{\infty} k \left[D_m J_{m+1}(kr) + E_m J_{m-1}(kr) \right] \quad (36)$$

$$b_z|_{|z|=0} = \frac{c}{2} \sum_{k=0}^{\infty} k (D_m + E_m) J_m(kr)$$

for $r > 1$

$$b_r|_{|z|=0} = \frac{i}{2} \sum_{k=0}^{\infty} k B_m \left[N_{m+1}(kr) - N_{m-1}(kr) \right]$$

$$b_{\varphi}|_{|z|=0} = -\frac{m}{r} \sum_{k=0}^{\infty} B_m N_m(kr)$$

$$b_z|_{|z|=0} = \frac{i}{2} \sum_{k=0}^{\infty} k B_m N_m(kr) \quad (37)$$

Inside and outside magnetic fields should be matched at the boundary of the disk, i.e. $r=1$. Matching \tilde{b}_r , \tilde{b}_{φ} and \tilde{b}_z respectively, one gets

$$D_m J_{m+1}(k) - E_m J_{m-1}(k) = 2 B_m \left(N_{m+1}(k) - \frac{m}{k} N_m(k) \right)$$

$$D_m J_{m+1}(k) + E_m J_{m-1}(k) = \frac{2m}{k} B_m N_m(k)$$

$$(D_m + E_m) J_m(k) = 2 B_m N_m(k) \quad (38)$$

Expressing from the 1st two equations C_m and A_m in terms of

B_m as:

$$D_m = B_m \frac{N_{m+1}(k)}{J_{m+1}(k)}$$

$$E_m = \frac{B_m \left[\frac{2m}{k} N_m(k) - N_{m+1}(k) \right]}{J_{m-1}(k)}$$

and plugging it in the 3rd equation of equation (38); one gets a dispersion relation:

$$N_{m+1}(k) \sigma_{m-1}(k) \sigma_m(k) + N_{m-1}(k) \sigma_{m+1}(k) \sigma_m(k) - 2 N_m(k) \sigma_{m+1}(k) \sigma_{m-1}(k) = 0 \quad (38')$$

From where, one gets the following dispersion relations for different m-modes: m=0

$$\mathcal{T}_1(k) = 0$$

m=1

$$N_2(k) \mathcal{T}_0(k) \mathcal{T}_1(k) + N_0(k) \mathcal{T}_2(k) \mathcal{T}_1(k) - 2 N_1(k) \mathcal{T}_2(k) \times \mathcal{T}_0(k) = 0$$

m=2

$$N_3(k) \mathcal{T}_1(k) \mathcal{T}_2(k) + N_1(k) \mathcal{T}_3(k) \mathcal{T}_2(k) - 2 N_2(k) \mathcal{T}_3(k) \times \mathcal{T}_1(k) = 0$$

The zeros of the above equations have been tabulated in Table 2.1.

2.10. Global Eigenvalue Equation

The set of MHD equations (1)-(7) can be written in a more appropriate form to allow some simplifications in equations and consequent reduction in the computing time. We add and subtract r and φ component of equation of motion to get the following two equations involving the quantities

$$\tilde{v}_r + i \tilde{v}_\varphi \text{ and } \tilde{v}_r - i \tilde{v}_\varphi :$$

$$\begin{aligned} i \nu (\tilde{v}_r + i \tilde{v}_\varphi) + 2 i (\tilde{v}_r + i \tilde{v}_\varphi) + \frac{\tilde{\sigma}}{\sigma_0} \left(\frac{1}{r^2} - r \right) = \\ = - \frac{1}{\sigma_0} \left(\frac{d \tilde{p}}{d r} + \frac{m}{r} \tilde{p} \right) + \frac{2 B_{0z}}{\sigma_0} (\tilde{b}_r + i \tilde{b}_\varphi) + \frac{2 B_{0r}}{\sigma_0} \tilde{b}_z \end{aligned}$$

$$i\omega(\tilde{v}_r - i\tilde{v}_\varphi) - 2i(\tilde{v}_r - i\tilde{v}_\varphi) = -\frac{1}{\sigma_0} \left(\frac{d\tilde{p}}{dr} - \frac{m}{r} \tilde{p} \right) + \\ + \frac{2B_{0z}}{\sigma_0} (\tilde{b}_r - i\tilde{b}_\varphi) + \frac{2B_{0r}}{\sigma_0} \tilde{b}_z$$

Similarly, adding and subtracting r and φ component of the induction equation, one gets the quantities involving

$$\tilde{b}_r + i\tilde{b}_\varphi \text{ and } \tilde{b}_r - i\tilde{b}_\varphi$$

$$i\omega(\tilde{b}_r + i\tilde{b}_\varphi) = -\frac{B_{0r}}{r} (\tilde{v}_r + i\tilde{v}_\varphi) - \tilde{v}_r \frac{dB_{0r}}{dr} + \\ + iB_{0r} \left(\frac{d\tilde{v}_\varphi}{dr} + \frac{m}{r} \tilde{v}_\varphi \right)$$

$$i\omega(\tilde{b}_r - i\tilde{b}_\varphi) = -\frac{B_{0r}}{r} (\tilde{v}_r - i\tilde{v}_\varphi) - \tilde{v}_r \frac{dB_{0r}}{dr} - \\ - iB_{0r} \left(\frac{d\tilde{v}_\varphi}{dr} - \frac{m}{r} \tilde{v}_\varphi \right)$$

where,

$$\tilde{\omega} = \omega - m\Omega_0$$

Therefore, after rearranging the equations, as pointed out above, one gets the following set of equations:

$$\begin{aligned} i\tilde{\omega}\tilde{\sigma} + \frac{1}{r} \left[\frac{d}{dr} (r\tilde{v}_r\sigma_0) - im\sigma_0\tilde{v}_\varphi \right] &= 0 \\ i\omega(\tilde{v}_r + i\tilde{v}_\varphi) + 2i(\tilde{v}_r + i\tilde{v}_\varphi) + \frac{\tilde{\sigma}}{\sigma_0} \left(\frac{1}{r^2} - r \right) &= \\ = -\frac{1}{\sigma_0} \left(\frac{d\tilde{p}}{dr} + \frac{m}{r} \tilde{p} \right) + \frac{2B_{0z}}{\sigma_0} (\tilde{b}_r + i\tilde{b}_\varphi) + \frac{2B_{0r}}{\sigma_0} \tilde{b}_z & \\ i\omega(\tilde{v}_r - i\tilde{v}_\varphi) - 2i(\tilde{v}_r - i\tilde{v}_\varphi) = -\frac{1}{\sigma_0} \left(\frac{d\tilde{p}}{dr} - \frac{m}{r} \tilde{p} \right) + & \\ + \frac{2B_{0z}}{\sigma_0} (\tilde{b}_r - i\tilde{b}_\varphi) + \frac{2B_{0r}}{\sigma_0} \tilde{b}_z & \end{aligned} \quad (39)$$

$$i v (\tilde{b}_r + i \tilde{b}_\varphi) = - \frac{B_{0r}}{r} (\tilde{v}_r + i \tilde{v}_\varphi) - \tilde{v}_r \frac{dB_{0r}}{dr} + \left. \begin{aligned} &+ i B_{0r} \left(\frac{d\tilde{v}_\varphi}{dr} + \frac{m}{r} \tilde{v}_\varphi \right) \end{aligned} \right\} \quad (39)$$

$$i v (\tilde{b}_r - i \tilde{b}_\varphi) = - \frac{B_{0r}}{r} (\tilde{v}_r - i \tilde{v}_\varphi) - \tilde{v}_r \frac{dB_{0r}}{dr} - \left. \begin{aligned} &- i B_{0r} \left(\frac{d\tilde{v}_\varphi}{dr} - \frac{m}{r} \tilde{v}_\varphi \right) \end{aligned} \right\} \quad (40)$$

We expand the radial and azimuthal component of the magnetic field as in equation (36) while the density and the quantities $\tilde{v}_r + i \tilde{v}_\varphi$ and $\tilde{v}_r - i \tilde{v}_\varphi$ are written as:

$$\begin{aligned} \phi(r) &= \sum_{k=0}^{\infty} A_m J_m(kr) \\ \tilde{v}_r + i \tilde{v}_\varphi &= i \sum_{k=0}^{\infty} B_m J_{m+1}(kr) \\ \tilde{v}_r - i \tilde{v}_\varphi &= i \sum_{k=0}^{\infty} C_m J_{m-1}(kr) \end{aligned} \quad (41)$$

Which yields for the radial part of the perturbed components \tilde{v}_r and \tilde{v}_φ

$$\begin{aligned} \tilde{v}_r &= \frac{i}{2} \sum_{k=0}^{\infty} B_m J_{m+1}(kr) + C_m J_{m-1}(kr) \\ \tilde{v}_\varphi &= \frac{1}{2} \sum_{k=0}^{\infty} B_m J_{m+1}(kr) - C_m J_{m-1}(kr) \end{aligned}$$

From (36),

$$\begin{aligned}\tilde{b}_r + i\tilde{b}_\varphi &= -i \sum_{k=0}^{\infty} k E_m \mathcal{T}_{m-1}(kr) \\ \hat{b}_r - i\hat{b}_\varphi &= i \sum_{k=0}^{\infty} k D_m \mathcal{T}_{m+1}(kr)\end{aligned}\quad (36')$$

Plugging (41) and (36') in equation (39)-(40), one gets an infinite set of equations as follows:

$$\begin{aligned}& \mathcal{V} \sum_{k=0}^{\infty} A_m \mathcal{T}_m(kr) + \sum_{k=0}^{\infty} B_m \left[\mathcal{T}_{m+1}(kr) \left(\frac{1}{2} \frac{d\sigma_0}{d\gamma} - \frac{m\sigma_0}{\gamma} \right) + \right. \\ & \left. + \frac{k\sigma_0}{2} \mathcal{T}_m(kr) \right] + \sum_{k=0}^{\infty} C_m \left[\mathcal{T}_{m-1}(kr) \left(\frac{1}{2} \frac{d\sigma_0}{d\gamma} + \frac{\sigma_0}{\gamma} \right) + \right. \\ & \left. + \frac{k\sigma_0}{2} \mathcal{T}_{m-1}(kr) \right] = 0\end{aligned}\quad (43)$$

$$\begin{aligned}& -(\mathcal{V}+2) \sum_{k=0}^{\infty} B_m \mathcal{T}_{m+1}(kr) + \sum_{k=0}^{\infty} A_m \left[\left\{ \frac{(\frac{1}{r_2}-r)}{\sigma_0} + \frac{\gamma P \left(\frac{\delta-1}{\sigma_0^2} \right) \frac{d\sigma_0}{d\gamma}}{\sigma_0^2} \right\} \times \right. \\ & \left. \times \mathcal{T}_m(kr) + \frac{\gamma P_0}{\sigma_0^2} k \mathcal{T}_{m-1}(kr) \right] + \sum_{k=0}^{\infty} E_m \frac{2ik}{\sigma_0} B_{02} \mathcal{T}_{m-1}(kr) - \\ & - \sum_{k=0}^{\infty} \frac{ik}{\sigma_0} B_{07} (D_m + E_m) \mathcal{T}_m(kr) = 0\end{aligned}\quad (44)$$

$$\begin{aligned}& -(\mathcal{V}+2) \sum_{k=0}^{\infty} C_m \mathcal{T}_{m-1}(kr) + \sum_{k=0}^{\infty} A_m \frac{\gamma P_0}{\sigma_0^2} \left[k \mathcal{T}_{m-1}(kr) + \right. \\ & \left. + \left\{ \frac{\delta-1}{\sigma_0} \frac{d\sigma_0}{d\gamma} - \frac{2m}{\gamma} \right\} \mathcal{T}_m(kr) \right] - \sum_{k=0}^{\infty} \frac{ik}{\sigma_0} D_m \left[2B_{02} \mathcal{T}_{m+1}(kr) + \right. \\ & \left. + B_{07} \mathcal{T}_m(kr) \right] - \sum_{k=0}^{\infty} \frac{ik}{\sigma_0} B_{07} E_m \mathcal{T}_m(kr) = 0\end{aligned}\quad (45)$$

$$\begin{aligned}& \mathcal{V} \sum_{k=0}^{\infty} k E_m \mathcal{T}_{m-1}(kr) + \frac{iB_{07}}{\gamma} \sum_{k=0}^{\infty} B_m \mathcal{T}_{m+1}(kr) + \frac{i}{2} \frac{dB_{07}}{d\gamma} \sum_{k=0}^{\infty} \left[B_m \mathcal{T}_{m+1}(kr) + \right. \\ & \left. + C_m \mathcal{T}_{m-1}(kr) \right] - \frac{iB_{07}}{2} \sum_{k=0}^{\infty} \left[B_m \left\{ k \mathcal{T}_m(kr) - \frac{1}{\gamma} \mathcal{T}_{m+1}(kr) \right\} + \right. \\ & \left. + C_m \left\{ k \mathcal{T}_{m-2}(kr) + \frac{1}{\gamma} \mathcal{T}_{m-1}(kr) \right\} \right] = 0\end{aligned}\quad (46)$$

$$\begin{aligned}
 & - \nu \sum_{k=0}^{\infty} k D_m J_{m+1}(kr) + \frac{2B_0 r}{\gamma} \sum_{k=0}^{\infty} C_m J_{m-1}(kr) + \frac{\ell}{2} \frac{dB_0}{dr} \sum_{k=0}^{\infty} \left[B_m \right. \\
 & \times J_{m+1}(kr) + C_m J_{m-1}(kr) \left. \right] + \frac{2B_0 r}{2} \sum_{k=0}^{\infty} \left[B_m \left\{ k J_m(kr) - \right. \right. \\
 & \left. \left. - \frac{2m+1}{\gamma} J_{m+1}(kr) \right\} - C_m \left\{ k J_{m-2}(kr) - \frac{2m-1}{\gamma} J_{m-1}(kr) \right\} \right] = 0 \quad (47)
 \end{aligned}$$

Now, multiplying the above equations (43), (44), (45), (46) and (47) by $\gamma J_m(\ell r)$, $\gamma J_{m+1}(\ell r)$, $\gamma J_{m-1}(\ell r)$, $\gamma J_m(\ell r)$, $\gamma J_{m+1}(\ell r)$ respectively and integrating over the disk, one gets the following algebraic equations:

$$\begin{aligned}
 m \sum_{\ell=0}^{\infty} A_m^{\ell} + \sum_{k, \ell=0}^{\infty} B_m^k \beta_{k\ell} + \sum_{k, \ell=0}^{\infty} C_m^k \chi_{k\ell} &= \omega \sum_{\ell=0}^{\infty} A_m^{\ell} \\
 (m-2) \sum_{\ell=0}^{\infty} B_m^{\ell} + \sum_{k, \ell=0}^{\infty} A_m^k \alpha_{k\ell} + \sum_{k, \ell=0}^{\infty} E_m^k \epsilon_{k\ell} + \sum_{k, \ell=0}^{\infty} D_m^k \delta_{k\ell} &= \\
 &= \omega \sum_{\ell=0}^{\infty} B_m^{\ell} \\
 (m+2) \sum_{\ell=0}^{\infty} C_m^{\ell} + \sum_{k, \ell=0}^{\infty} A_m^k \alpha_{k\ell}^{(1)} + \sum_{k, \ell=0}^{\infty} D_m^k \delta_{k\ell}^{(1)} + \sum_{k, \ell=0}^{\infty} E_m^k \epsilon_{k\ell}^{(1)} &= \\
 &= \omega \sum_{\ell=0}^{\infty} C_m^{\ell} \\
 m \sum_{\ell=0}^{\infty} E_m^{\ell} + \sum_{k, \ell=0}^{\infty} B_m^k \beta_{k\ell}^{(1)} + \sum_{k, \ell=0}^{\infty} C_m^k \chi_{k\ell}^{(1)} &= \omega \sum_{\ell=0}^{\infty} E_m^{\ell} \\
 m \sum_{\ell=0}^{\infty} D_m^{\ell} + \sum_{k, \ell=0}^{\infty} B_m^k \beta_{k\ell}^{(2)} + \sum_{k, \ell=0}^{\infty} C_m^k \chi_{k\ell}^{(2)} &= \omega \sum_{\ell=0}^{\infty} D_m^{\ell}
 \end{aligned}$$

Where,

$$\begin{aligned}
 \beta_{k\ell} &= - \frac{1}{M_1} \int_0^1 r dr J_m(\ell r) \left\{ J_{m+1}(kr) \left(\frac{1}{2} \frac{d\phi_0}{dr} + \frac{m\phi_0}{r} \right) + \right. \\
 & \quad \left. + \frac{k\phi_0}{2} J_m(kr) \right\} \\
 \chi_{k\ell} &= - \frac{1}{M_1} \int_0^1 r dr J_m(\ell r) \left\{ J_{m-1}(kr) \left(\frac{1}{2} \frac{d\phi_0}{dr} + \frac{m\phi_0}{r} \right) + \frac{k\phi_0}{2} J_{m-2}(kr) \right\}
 \end{aligned}$$

$$\alpha_{kl} = \frac{1}{M_2} \int_0^1 r dr J_{m+1}(kr) \left[\left\{ \frac{(\frac{1}{r} - r)}{\sigma_0} + \frac{\gamma(\gamma-1)p_0}{\sigma_0^3} \frac{d\sigma_0}{dr} \right\} J_m(kr) + \frac{\delta p_0}{\sigma_0^2} k J_{m-1}(kr) \right]$$

$$\epsilon_{kl} = \frac{ik}{M_2} \int_0^1 \frac{r dr}{\sigma_0} J_{m+1}(kr) \left[2B_{0z} J_{m-1}(kr) - B_{0r} J_m(kr) \right]$$

$$\delta_{kl} = -\frac{ik}{M_2} \int_0^1 \frac{r dr}{\sigma_0} J_{m+1}(kr) B_{0r}(r) J_m(kr)$$

$$\alpha_{kl}^{(1)} = \frac{\gamma}{M_3} \int_0^1 r dr J_{m-1}(kr) \left[k J_{m-1}(kr) + \left\{ \frac{(\gamma-1)}{\sigma_0} \frac{d\sigma_0}{dr} - \frac{2m}{r} \right\} J_m(kr) \right] \frac{p_0}{\sigma_0^2}$$

$$\delta_{kl}^{(1)} = -\frac{ik}{M_3} \int_0^1 \frac{r dr}{\sigma_0} J_{m-1}(kr) \left[2B_{0z} J_{m+1}(kr) + B_{0r} J_m(kr) \right]$$

$$\epsilon_{kl}^{(1)} = -\frac{ik}{M_3} \int_0^1 \frac{r dr}{\sigma_0} J_{m-1}(kr) B_{0r} J_m(kr)$$

$$\beta_{kl}^{(1)} = \frac{-i}{KM_3} \int_0^1 r dr J_{m-1}(kr) \left[J_{m+1}(kr) \left\{ \frac{2}{r} B_{0r} + \frac{1}{2} \frac{dB_{0r}}{dr} \right\} - \frac{k B_{0r}}{2} J_m(kr) \right]$$

$$\chi_{kl}^{(1)} = \frac{-i}{2KM_3} \int_0^1 r dr J_{m-1}(kr) \left[\left(\frac{B_{0r}}{r} + \frac{dB_{0r}}{dr} \right) J_{m-1}(kr) + k B_{0r} J_{m-2}(kr) \right]$$

$$\beta_{kl}^{(2)} = \frac{i}{2KM_2} \int_0^1 r dr J_{m+1}(kr) \left[\left\{ \frac{dB_{0r}}{dr} - \frac{(2m+1)B_{0r}}{r} \right\} J_{m+1}(kr) + k B_{0r} J_m(kr) \right]$$

$$\chi_{kl}^{(2)} = \frac{i}{2KM_2} \int_0^1 r dr J_{m+1}(kr) \left[\left\{ \frac{dB_{0r}}{dr} + \frac{(2m+1)B_{0r}}{r} \right\} J_{m-1}(kr) - k B_{0r} J_{m-2}(kr) \right] \quad (48)$$

$$M_1 = \frac{1}{2} \{ J_{m+1}(l) \}^2, \quad M_2 = \frac{1}{2} \{ J_{m+2}(l) \}^2, \quad M_3 = \frac{1}{2} \{ J_m(l) \}^2$$

The set of algebraic equations (48) can, conveniently be

written in a matrix form:

$$\begin{bmatrix} m & \beta_{ke} & \chi_{ke} & 0 & 0 \\ \alpha_{ke} & m-2 & 0 & \delta_{ke} & \epsilon_{ke} \\ \alpha_{ke}^{(1)} & 0 & m+2 & \delta_{ke}^{(1)} & \epsilon_{ke}^{(1)} \\ 0 & \beta_{ke}^{(2)} & \chi_{ke}^{(2)} & m & 0 \\ 0 & \beta_{ke}^{(1)} & \chi_{ke}^{(1)} & 0 & m \end{bmatrix} \begin{bmatrix} A_e \\ B_e \\ C_e \\ D_e \\ E_e \end{bmatrix} = \omega \begin{bmatrix} A_e \\ B_e \\ C_e \\ D_e \\ E_e \end{bmatrix}$$

or

$$M \vec{X} = \omega \vec{X}$$

(49)

which defines an eigenvalue problem with ω as the eigenfrequency for the allowed mode of oscillations of the disk in question and M , the corresponding eigenfunctions. In general, M is complex, infinite, nonsymmetric matrix, where submatrices β , χ , α are infinite matrices themselves. \vec{X} is an infinite column matrix representing the eigenfunctions. We may note here that the nonsymmetric matrix, M , cannot be reduced to a symmetric form by any transformations.

One can attempt to solve the eigenvalue problem (49) by using a sufficiently large, truncated form of M and X . However, while truncating, the convergence of the eigenvalue and eigenfunctions has to be ensured. An analytic solution of

the problem is not possible and use has to be made of numerical methods in order to obtain the eigenspectrum. Complex, nonsymmetric matrices allow complex conjugate pairs of eigenvalues. Complex eigenvalues are associated with complex eigenfunctions, hence, introduce radial phase shifts in the perturbation maxima at various distances from the centre of the disk. Thus, in general, the complex eigenmodes yield spiral like feature.

Let us consider the magnetic field perturbation:

$$\tilde{b}_r + i \tilde{b}_\varphi = \text{Re} [f(r) e^{i(\omega t + m\varphi)}]$$

where,

$$f(r) = \sum_{k=0}^{\infty} E_j J_{m-1}(kr) = \sum_{k=0}^{\infty} (E_{j,\text{real}} + i E_{j,\text{imag}}) \times J_{m-1}(kr) = H_r + i H_i$$

Therefore,

$$\tilde{b}_r + i \tilde{b}_\varphi = \sqrt{(H_r^2 + H_i^2)} \cos(\omega t + m\varphi + \Phi(r))$$

where,

$$H_r = \sum_{k=0}^{\infty} E_{j,\text{real}} J_{m-1}(kr)$$

$$H_i = \sum_{k=0}^{\infty} E_{j,\text{imag}} J_{m-1}(kr)$$

and

$$\Phi(r) = \tan^{-1} (H_i/H_r)$$

If the amplitude part $[H_r^2 + H_i^2]^{1/2}$ is reasonably constant over the entire disk, the phase part at any instant of time, traces out a regular spiral for the maxima, described by

$$m\varphi + \Phi(r) = \text{Constant}$$

and other spiral branches at angles shifted by $2\pi/m$ for

$m > 0$. In almost all the cases, it is found that the amplitude part does not behave smoothly with r , so there are significant undulations. To study the allowed patterns in a more convenient manner, we have plotted the \tilde{b}_r and \tilde{b}_φ given by equation (36) as contour plots and three-dimensional plots. The field-perturbations at a large number of mesh points in- and out-side the disk have been generated using the eigenfunction in the equation (49).

Here, one may note that if the expansions in the equation (48) for the perturbed quantity retain n terms, the resulting eigenvalue problem would admit the normal mode with a maximum of $(n-1)$ modes in the range $0 \leq r \leq 1$ and the subsequent short-wavelength modes would not appear. By increasing the number of the terms in the expansion, the values of the existing eigenmodes would be refined, as well as, few more new short wavelength modes would be obtained. However, before the results for a particular mode are confidently discussed, its convergence with increasing dimension of the eigenmatrix in the equation (49) has to be checked.

2.11. Results and Discussions

We have carried out an analysis of the eigenvalue problem of a magnetized, gravitating, finite disk. A particular current density has been considered. However, in the formalism developed, any current density profile can be constructed in terms of a Bessel series and corresponding

magnetic field can be obtained by using equation (11).

The rotational profile is shown in figure (2.3) for different angular velocity. There is no differential rotation throughout the disk and the material revolves around the center as a solid body. Equilibrium magnetic fields B_r and B_z calculated using the equation (11) are shown in figure 2.4 along with the rotational velocity, for a fixed angular velocity. Equilibrium density distribution is calculated self-consistently from the radial equilibrium in the disk and is shown in figure 2.2.

2.11.1. The Eigen-Modes in Disk-Bulge System

The eigenvalue problem (49) has been solved with suitable truncations of the infinite dimensional matrix M . The convergence of the eigen-frequencies for $m=1$ and $m=2$ modes, as the dimension of the matrix increases, is shown in table (2.2). The relative changes in real and imaginary parts of the eigenvalue ω , are defined by

$$\Delta \omega_r = \frac{\omega_r \left| \begin{smallmatrix} p & p \end{smallmatrix} \right| - \omega_r \left| \begin{smallmatrix} q & q \end{smallmatrix} \right|}{\omega_r \left| \begin{smallmatrix} p & p \end{smallmatrix} \right|}$$

and

$$\Delta \omega_i = \left| \frac{\omega_i \big|_{(p \times p)} - \omega_i \big|_{(q \times q)}}{\omega_i \big|_{(p \times p)}} \right|$$

where $g < p$ and p and q are the size of the truncated matrix. Using data from table (2.2), we see for the leading mode that

$$\Delta \omega_r = 0.23528180 E+04 ; \Delta \omega_i = 0.17376263 E+04$$

for $m=1$

$$\Delta \omega_r = 0.53609618 E+03 ; \Delta \omega_i = 0.33129311 E+03$$

for $m=2$

thus, the relative error is not so small i.e. the convergence is not very good. As the dimension of the matrix is increased to larger values, numerical errors associated with the eigenvalue routine become significant. In view of these considerations we have adopted $n_t = 75$ for $m=1$ and $m=2$. Thus, the modes with the number of nodes larger than 15 has not been incorporated in our studies.

Figures (2.4), (2.5), (2.6) and (2.7) show the contour and the eigenpatterns for the radial and azimuthal components of the magnetic field for $m=1$ mode and for the fastest growth rate. Figures (2.8) and (2.9) compares eigenpattern for radial magnetic field as obtained from 60×60 and 75×75 matrix for $m=1$ mode. Figures (2.10) and (2.11) show the eigenpattern for azimuthal magnetic field

for $m=1$ mode with 60×60 and (75×75) matrix. Clearly pattern does changes and hence, convergence is not satisfactory.

We find the dominant unstable mode for $m=1$. Growth rate decreases as radial wavelength of perturbation increases. Dominant mode corresponds to the global structure of the magnetic field.

The pattern-frequency and growth rates for the principle (or the fastest growing) mode, with $m=1$ and $m=2$ are listed in table (2.3). In all the cases, the growth rates are small as compared to the pattern frequencies given by $\Omega_p (\equiv -\frac{\omega_r}{m})$, and hence explosive instabilities are absent in the disk.

Let us consider some typical calculations for $m=1$ mode, for allowed pattern velocities are of spiral patterns and amplification period. Considering a typical disk with a mass, $m = 2.10^{11} M_0$ and radius, $R = 10^8$ kpc, the normalization coefficients are

$$\left[\frac{\pi G M_0}{R} \right]^{1/2} = 595 \text{ km/sec for velocity}$$

$$\left[\frac{\pi G M}{R^3} \right]^{1/2} = 74.4 \text{ km/sec-kpc } (\equiv 7.8 \times 10^{-8} \text{ yr}^{-1}) \text{ for}$$

angular velocity

Here $G = 0.45145 \times 10^{-38} \text{ kpc}^3 / M_0 \text{-Sec}^2$

The circular velocity at a distance of 8 kpc from the center for the disk is

$$74.43 \text{ km/sec-kpc.}$$

The growth rate ω_1 as for the fastest mode is:

$$\begin{aligned}\omega_1 &= 0.718324 \times 10^4 \times 7.8 \times 10^{-8} \text{ yr}^{-1} \\ &= 0.56 \times 10^{-3} \text{ yr}^{-1}\end{aligned}$$

$$\begin{aligned}\text{Therefore, } P_{\text{am}} (\text{amplification period} \times 10^{+9} \text{ years}) &= \\ &= 5.6 \times 10^5 \text{ years}\end{aligned}$$

As is evident from the amplification period, the magnetic field increases over the life-time of the galaxy by a large amount ($\sim e^{10^5}$). It points out towards the fact that the linear analysis carried out above might not be accurate enough and one has to achieve the better convergence to be confident about the growth rates.

The pattern frequency, and growth rate for the fastest growing mode with $m=2$, are listed in table (2.3). In all the cases the growth rates are significantly small as compared to the pattern frequencies Ω_2 . Figures (2.12), (2.13) and (2.14) correspond to the contour and 3-D plots of the radial and azimuthal component of the magnetic field respectively.

We would like to remark that eigenvalue problems in the form, discussed above, remove several difficulties pointed in Chapter I and also, provide a natural explanation of the origin and persistence of different spiral modes in a gravitating magnetized disk.

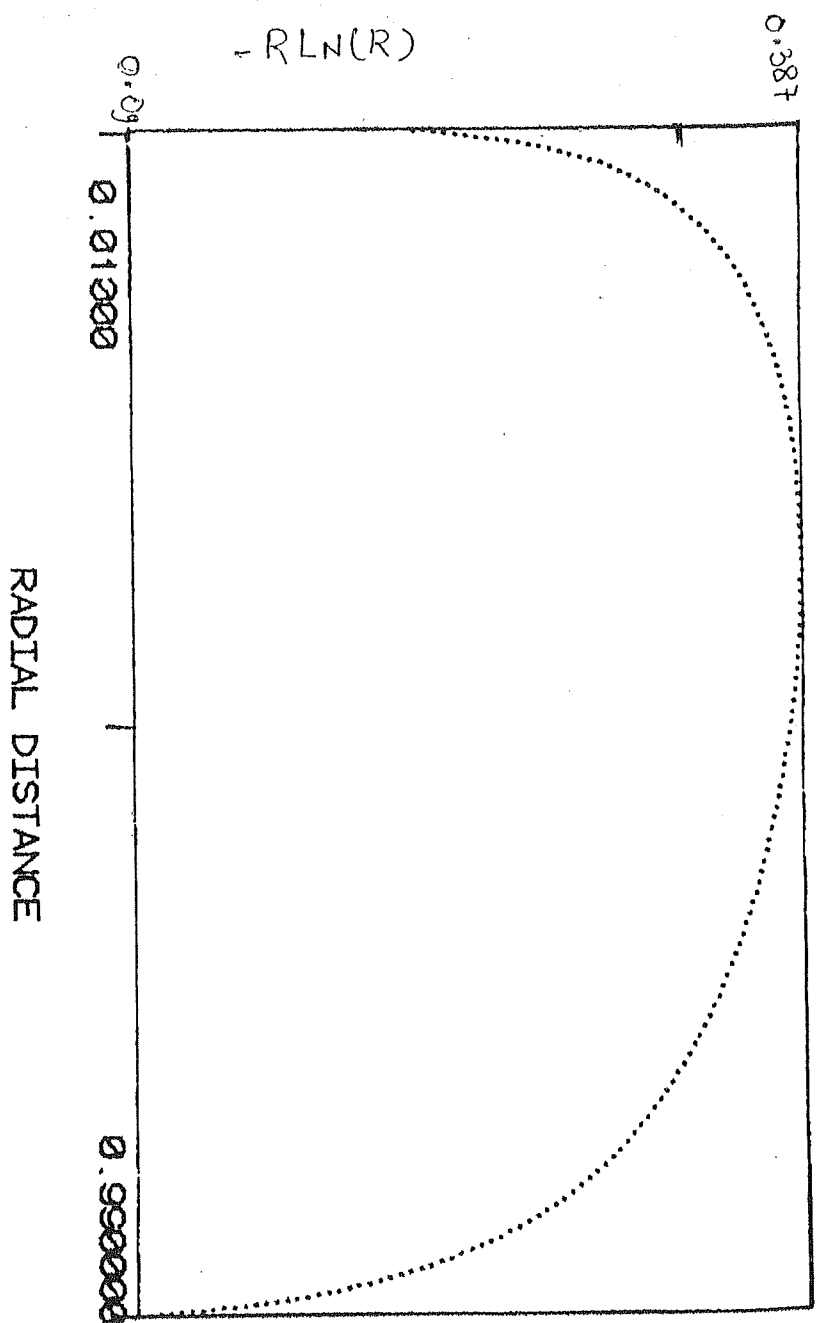


Fig. 2-1

EQUILIBRIUM DENSITY VS. RADIAL DISTANCE

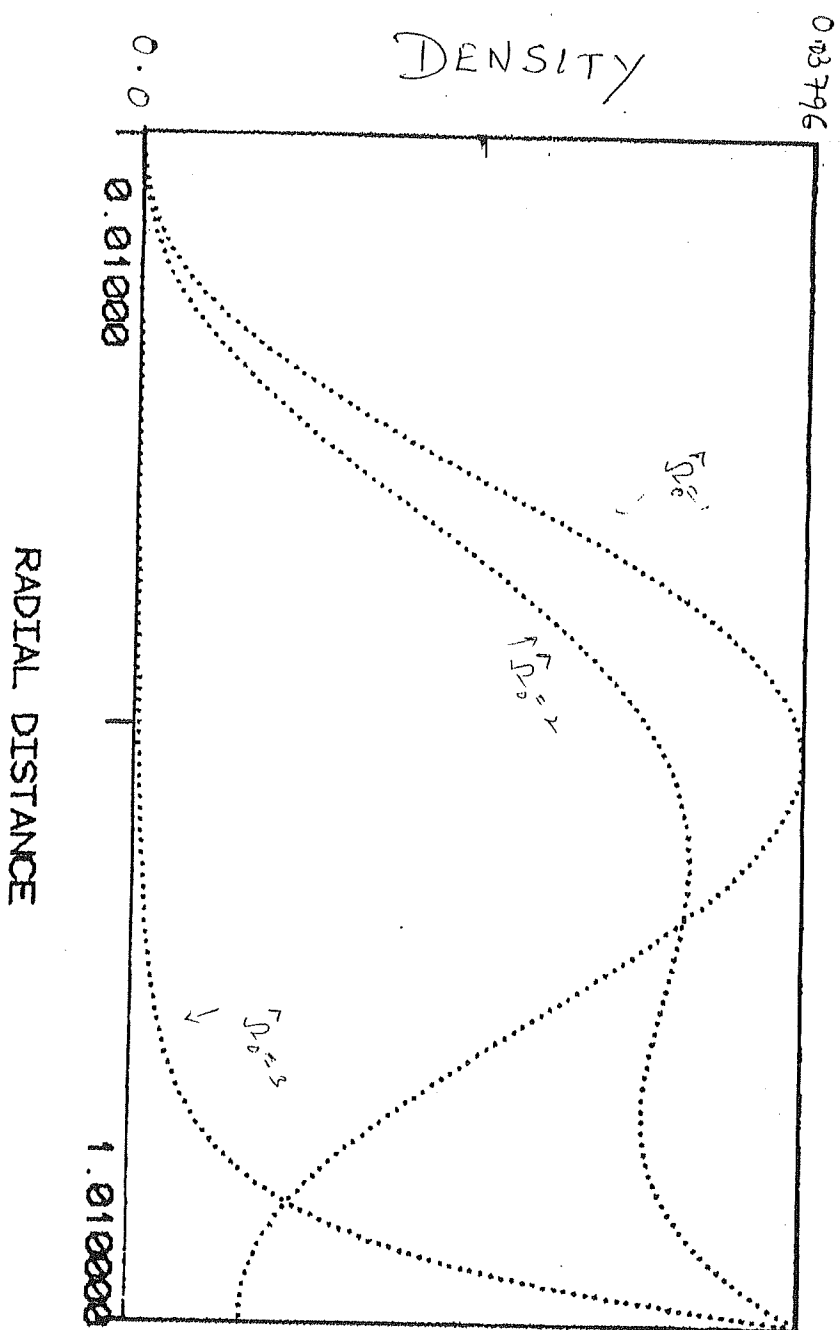


FIG. (2.2)

EQUILIBRIUM BR, BZ, V

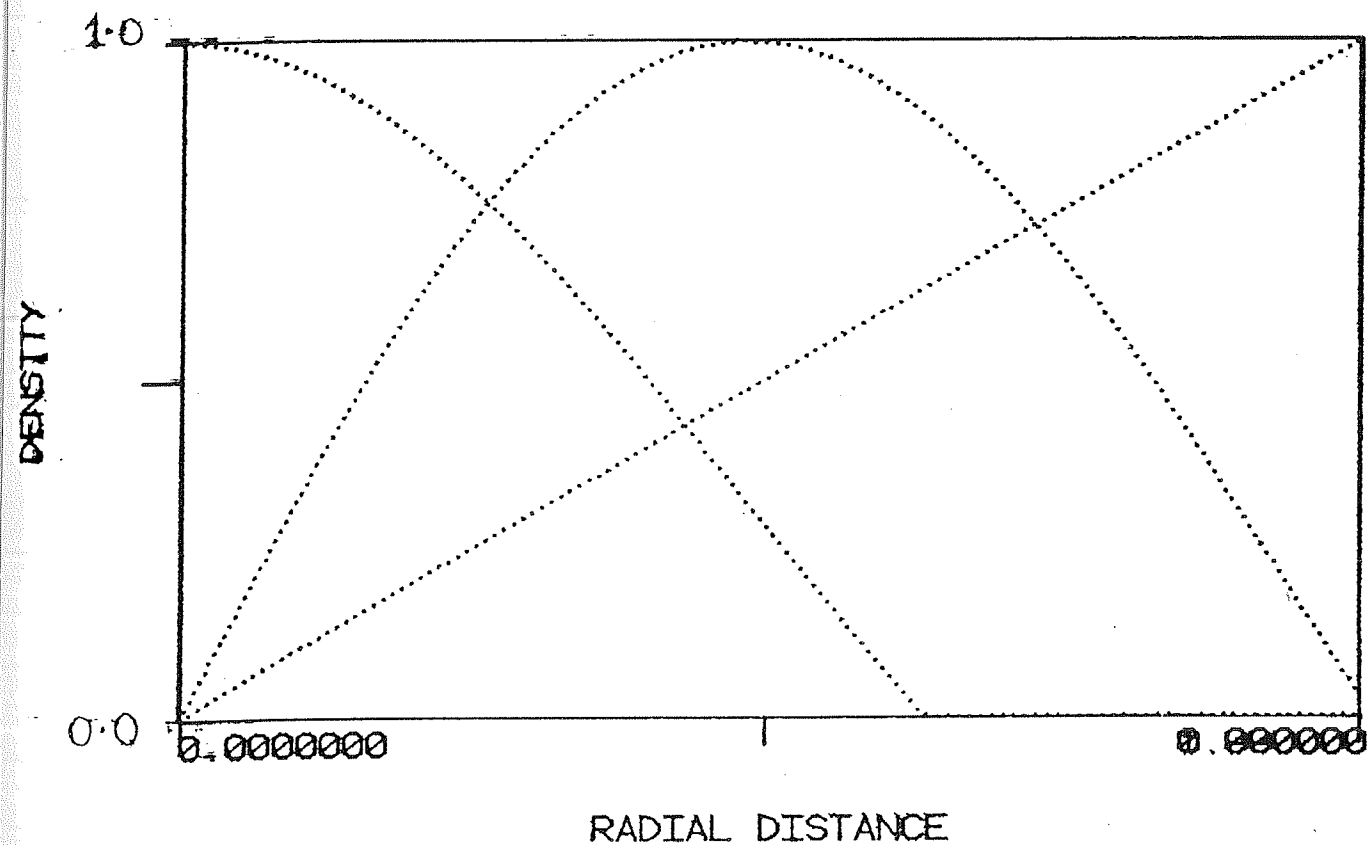


FIG. (2.3)

Radial Field Contour

75x75 matrix, $k = 11.70600$

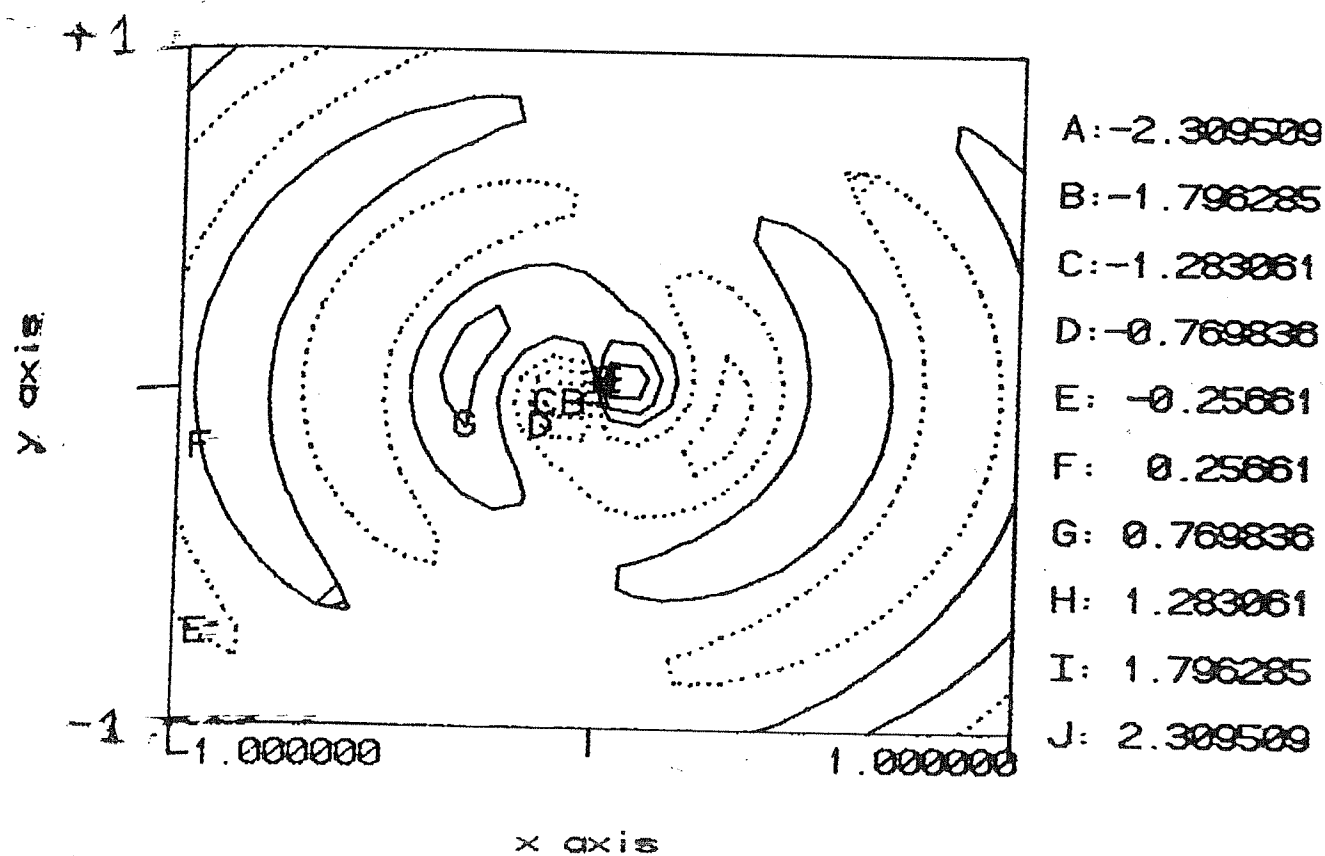
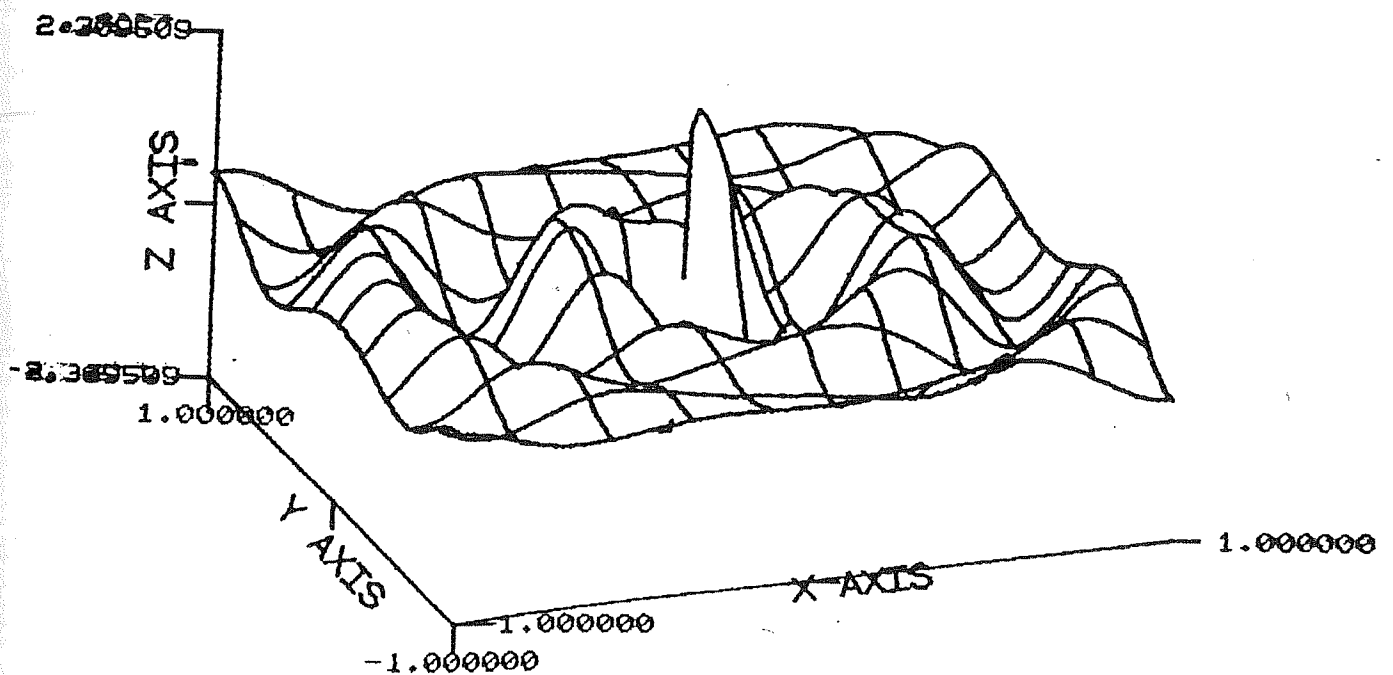


FIG.(2-4)

Radial Field Component

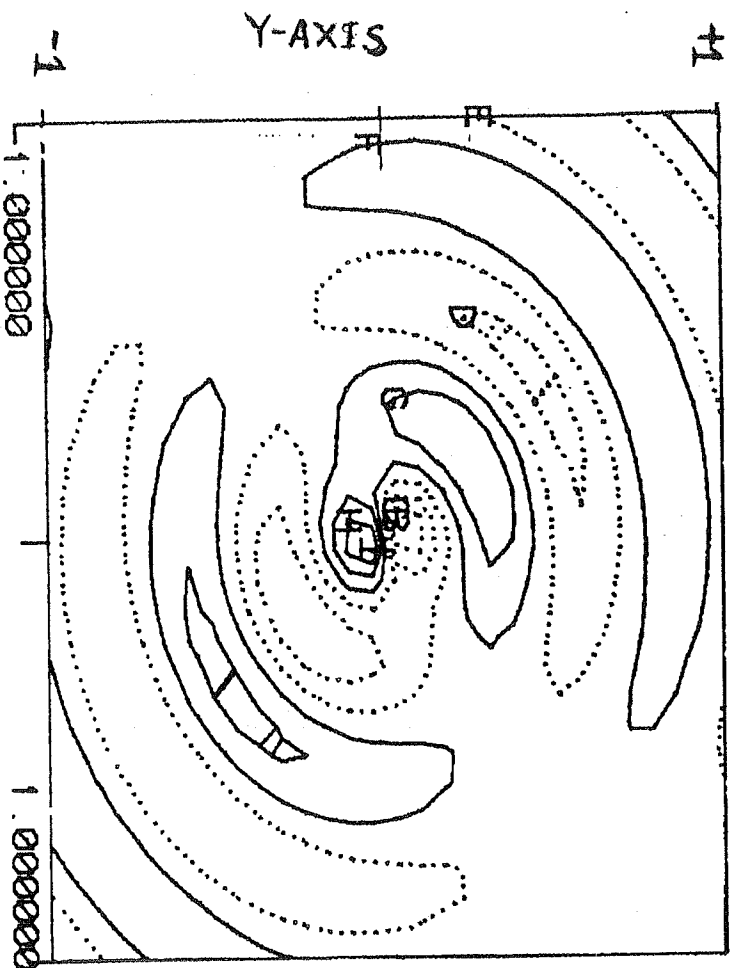
75x75 matrix ; $k=11.70600$



Fig(2.5)

Azimuthal Field Contour

75x75 matrix, $k=11.70600$



A: -2.294066

B: -1.784274

FIG (2.6)

Azimuthal Field Component

75x75 matrix ; $k = 11.70600$

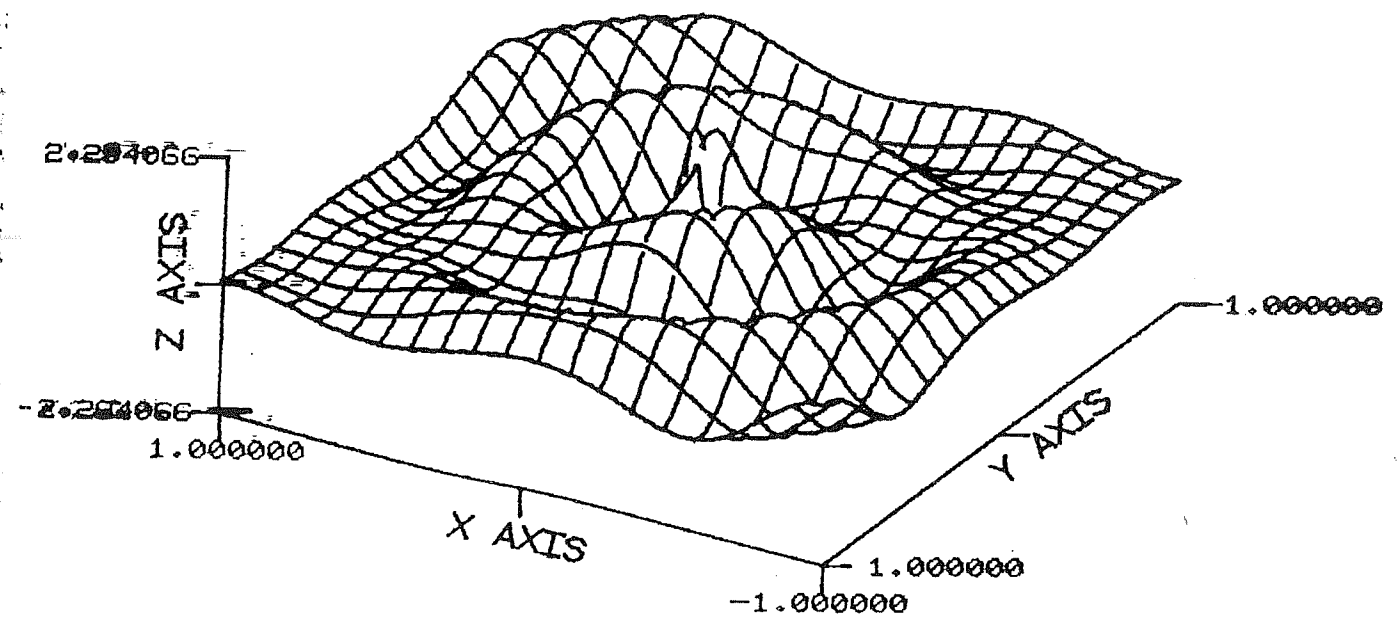


FIG.(2-7)

Radial Field Plot

60x60 matrix ; $k=11.70600$

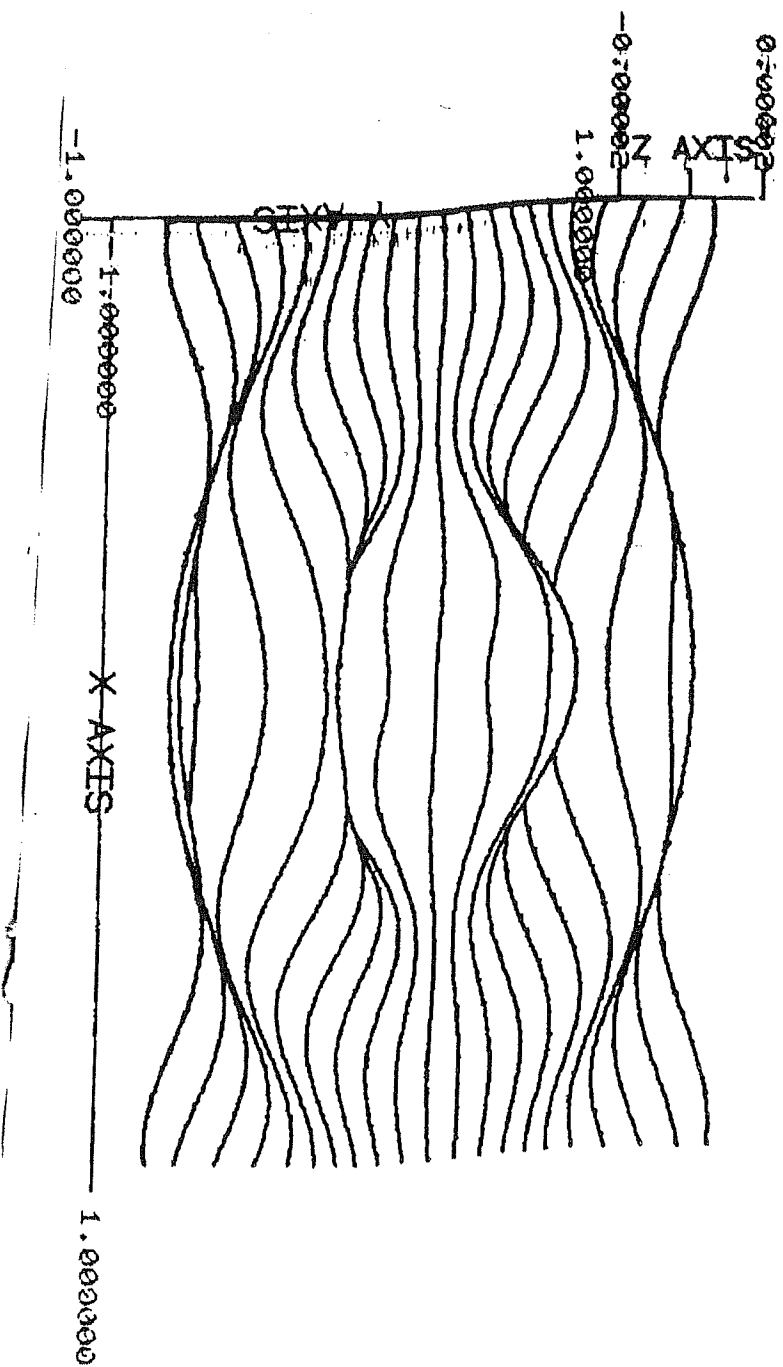


Fig. (2.8)

Radial Field Component

75x75 matrix ; $k = 11.70600$

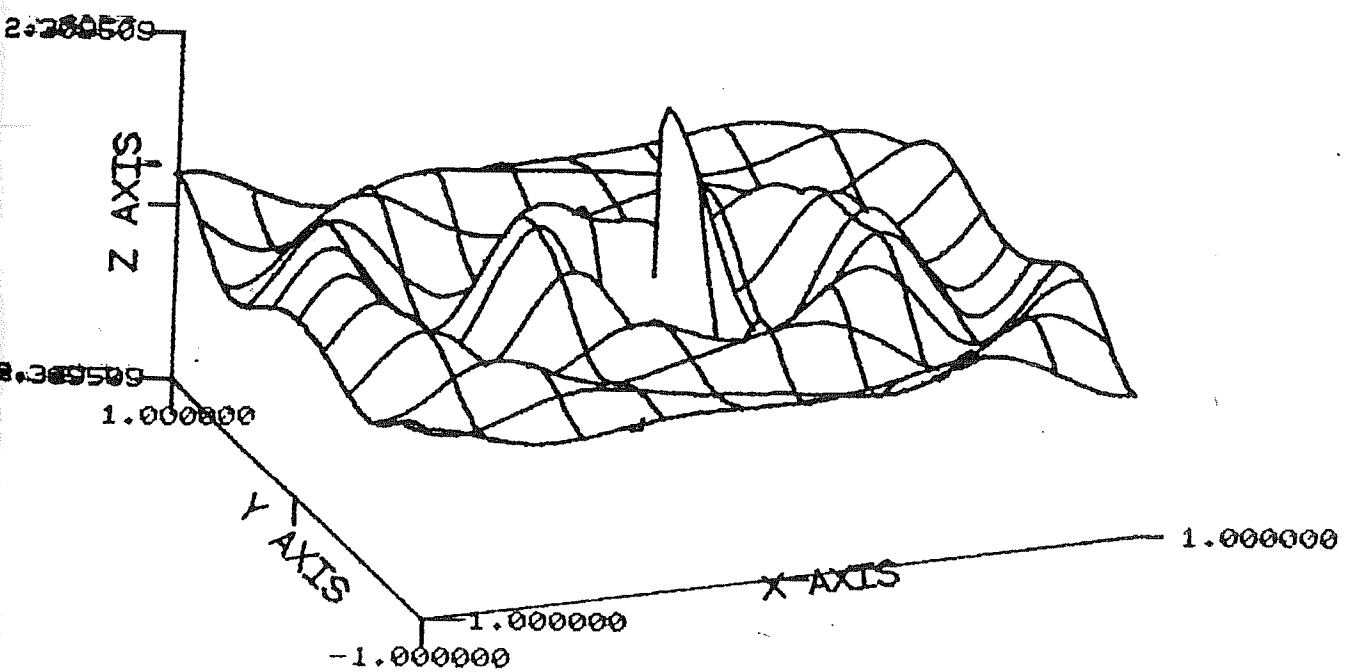


Fig.(2.9)

Azimuthal Field Component

60x60 matrix ; $k = 11.70600$

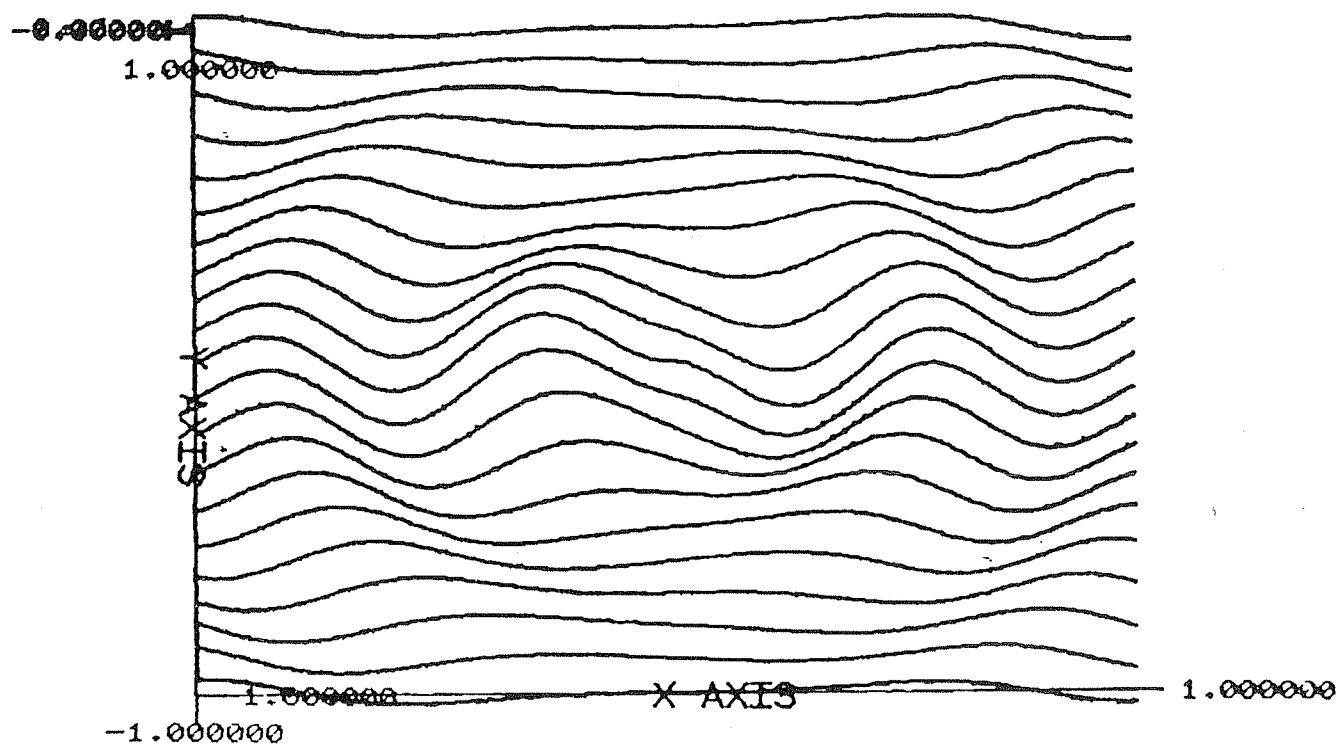


FIG. (2.10)

Azimuthal Field Component

75x75 matrix ; $k=11.46600$

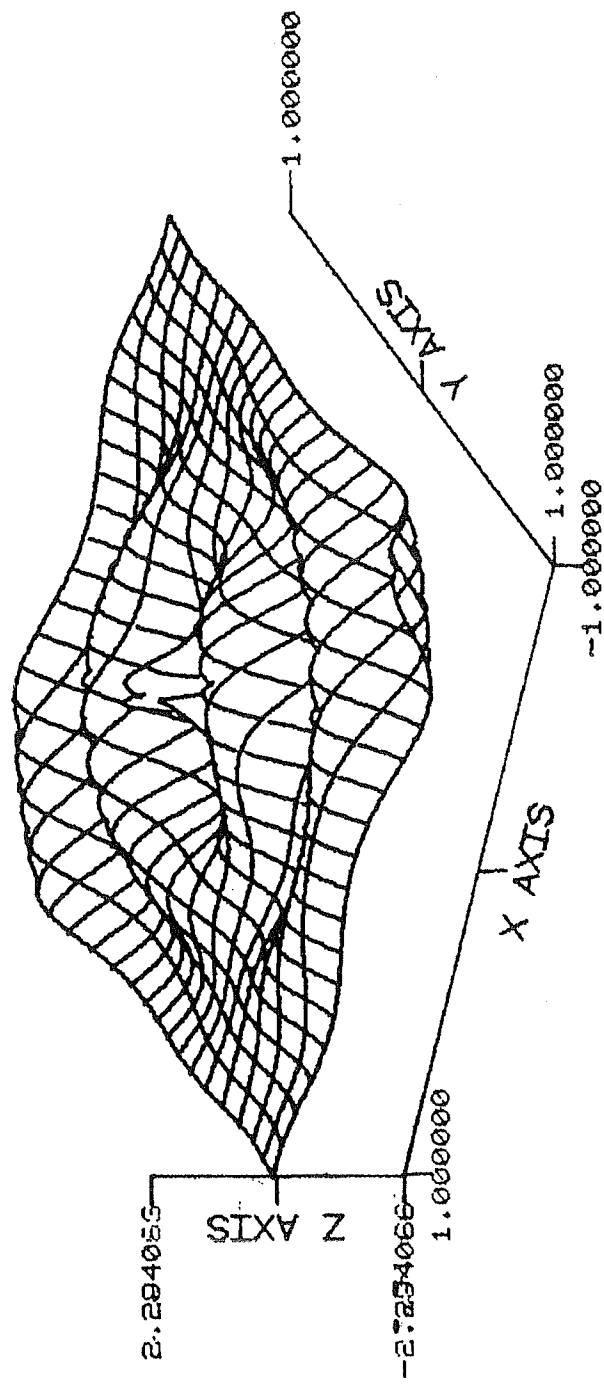


FIG.(2.11)

Radial Field Contour

75x75 matrix ; $k=13.17037$

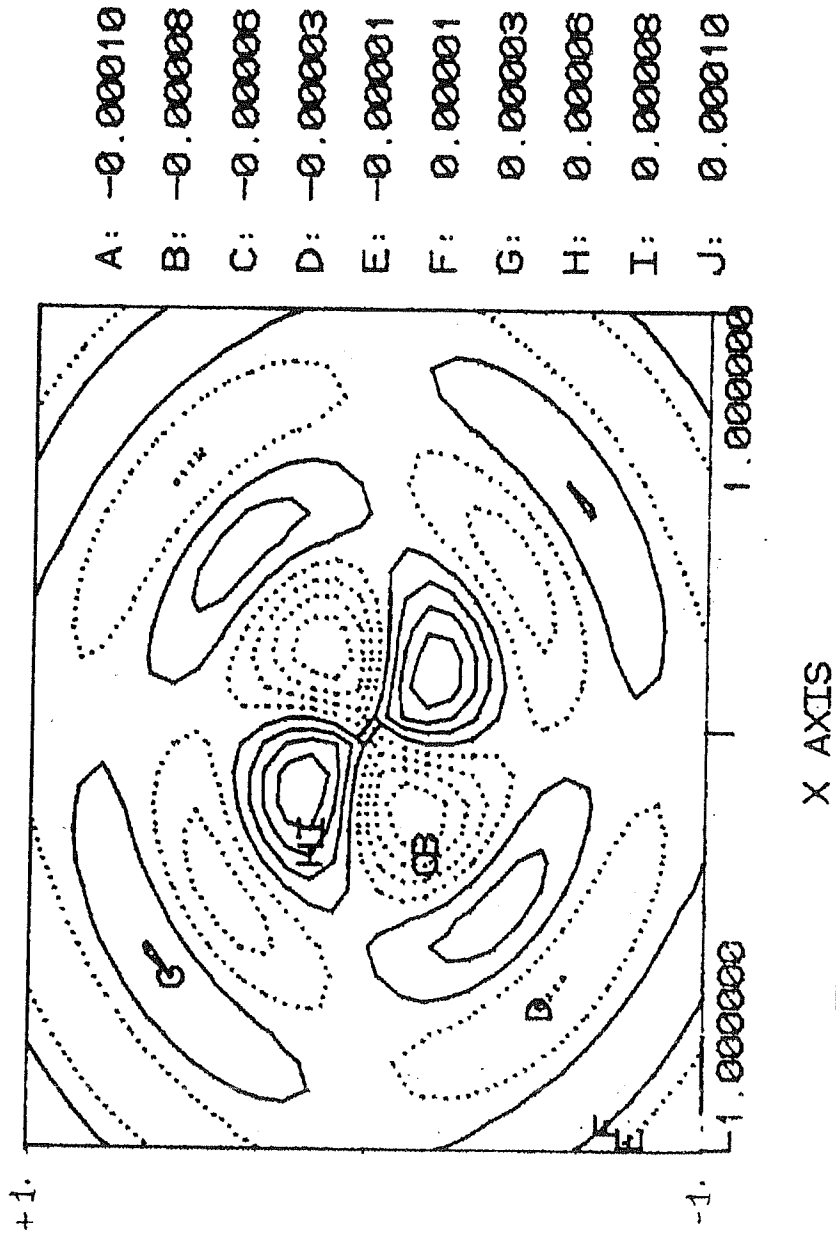


Fig.(2.12)

Radial Component Plot

$$k = 13.17037$$

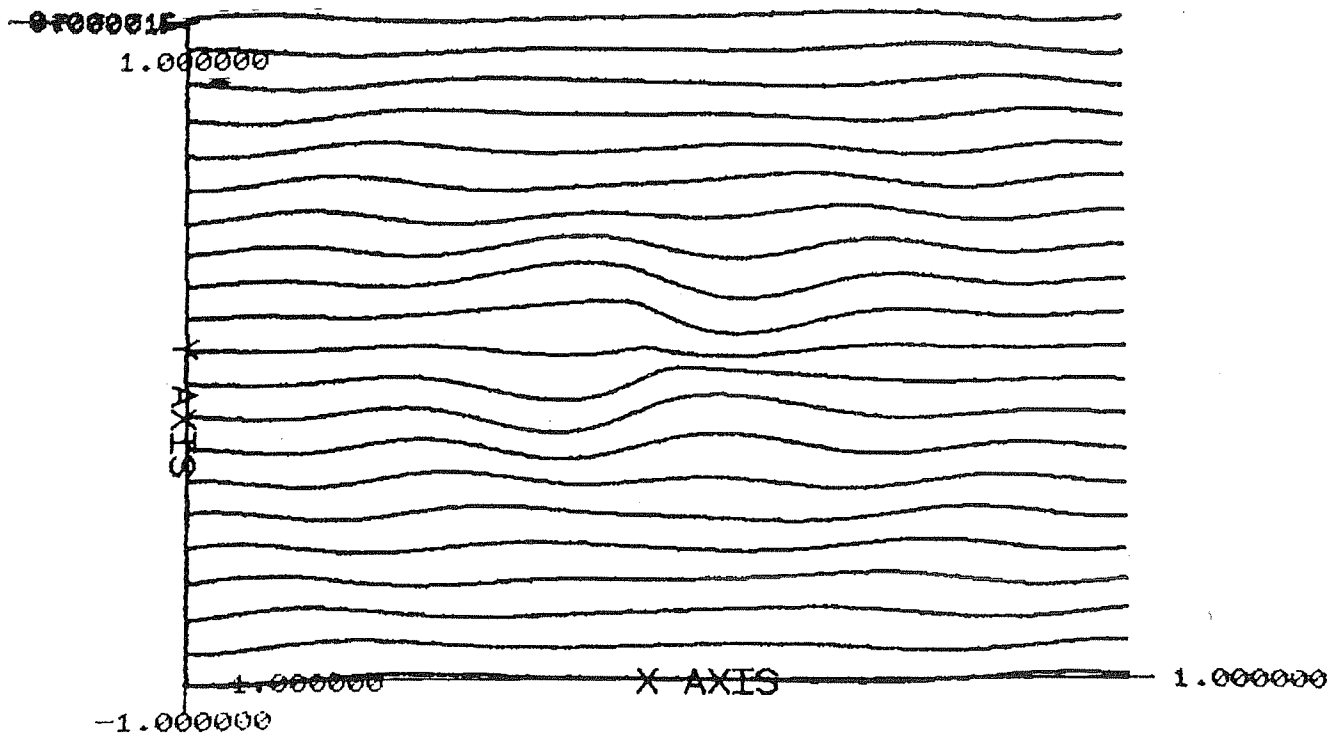


FIG. (2.13)

Azimuthal Component Plot

$$k = 13.47037$$

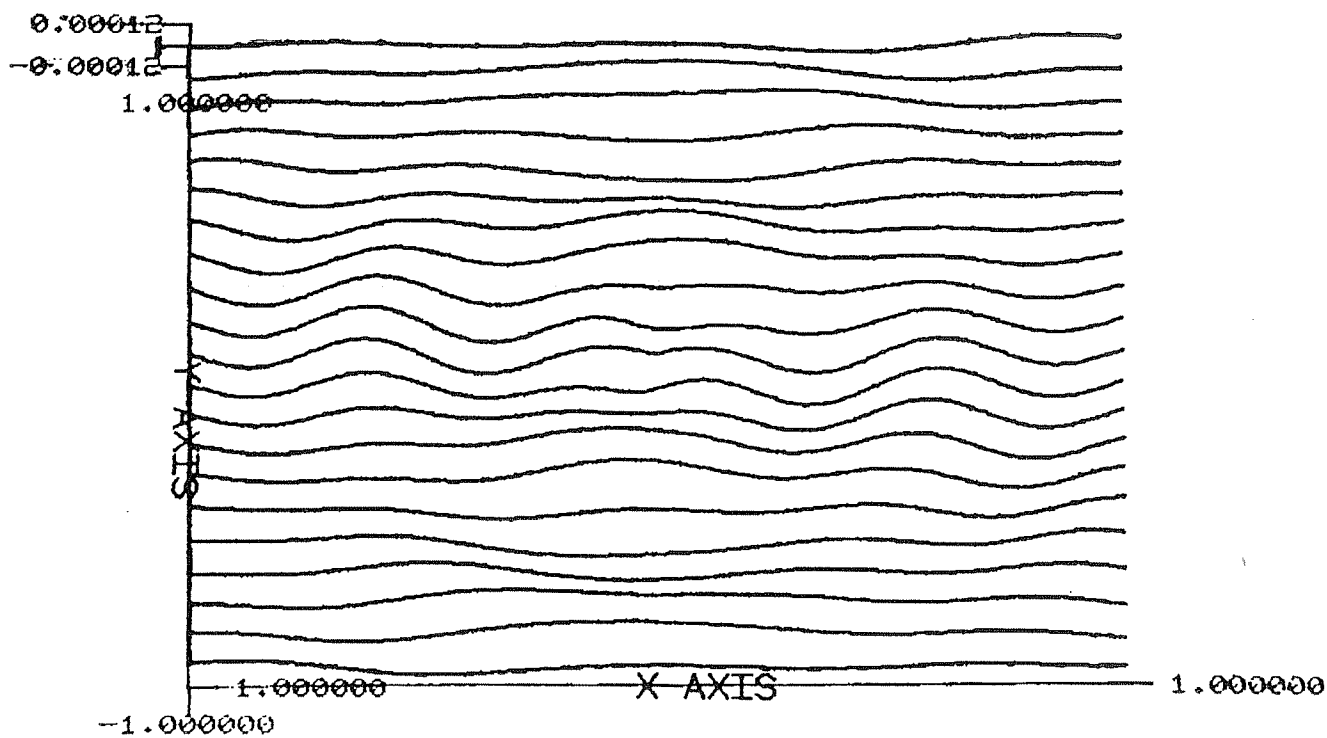


FIG. (2.14)

Azimuthal Component Contour (Corresponding to fig.2.14)

75x75 matrix ; $k = 13.47637$

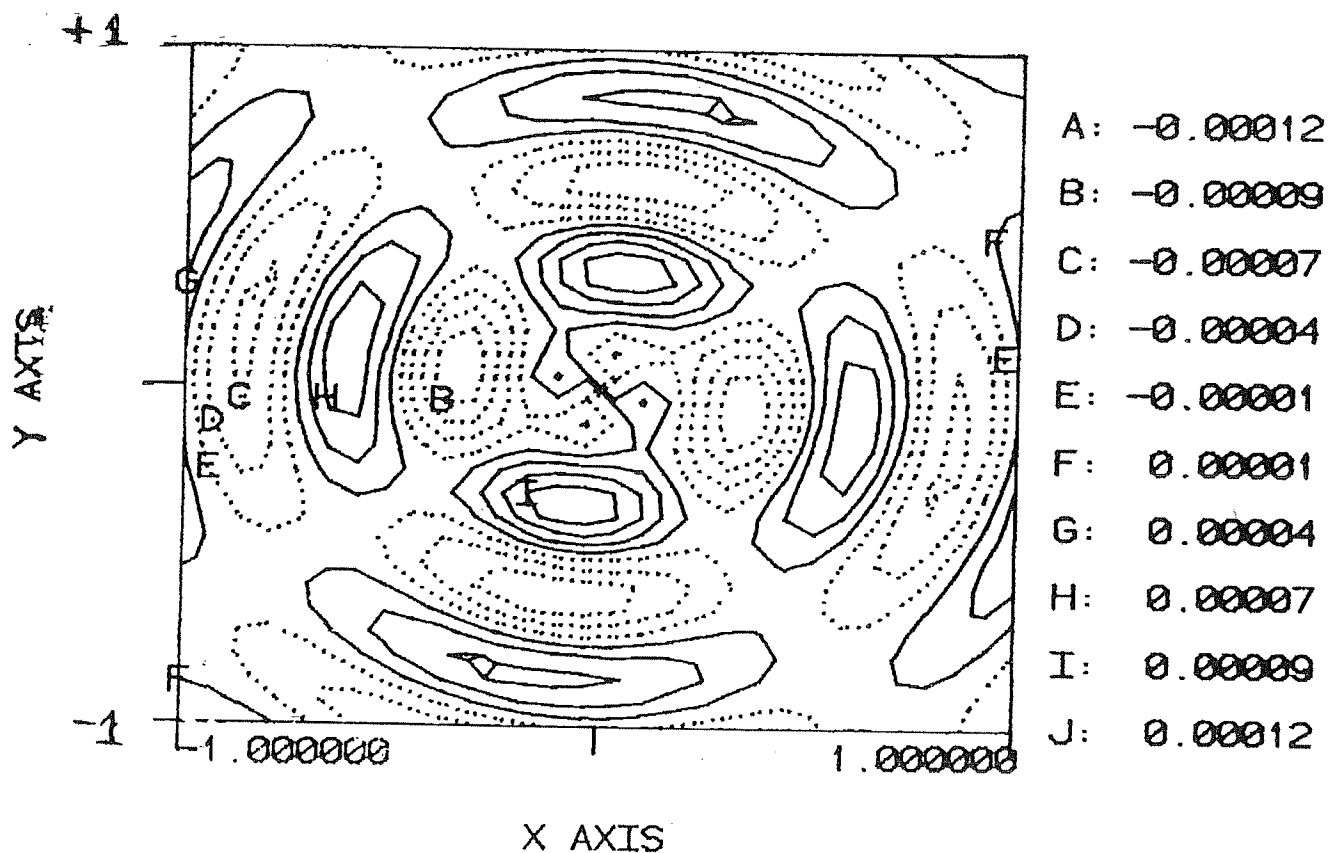


Table 2.1

First Fifteen Zeros of Dispersion Relation

m=1	m=2
1.841184	3.054237
5.331443	6.706133
8.536316	9.969468
11.70600	13.17037
14.86359	16.37752
18.01553	19.51291
21.16437	22.67158
24.31133	25.82604
27.45705	28.97767
30.60192	32.12733
33.74618	35.27554
36.88999	38.42266
40.03344	41.56894
43.17663	44.71455
46.31960	47.85964

Table 2.2

Principal Mode for Two Truncated Matrices

	(60x60)	(75x75)	(60x60)	(75x75)
m=1	3288.49	2353.46	4763.50	3025.87
m=2	866.19	328.57	1131.00	799.50

Table 2.3

Pattern Velocity and Growth Rate for (75x75) Matrix

m=1	-0.23531469 E+04	0.302587 E+04
m=2	-0.16428610 E+03	0.799500 E+03

CHAPTER III

NUMERICAL TECHNIQUES

3.1. Introduction

A large number of numerical schemes are involved in the analysis of the eigenvalue problems for the global modes in a magnetized, gravitating disk. We discuss, in this chapter,

the numerical methods we have employed for various calculations in the course of this work.

The eigen-matrices are, in general 500×500 matrices with matrix-elements, which themselves are certain integrals over the disk boundaries. In practice, however, one should truncate the size of the matrices involved to enable oneself to solve the problem by numerical methods. Truncation should be done after ensuring convergence of the eigenvalue and eigenfunctions. Here, we have discussed the numerical calculations involved to form the eigenmatrices in section 3.2. About eigenroutines, we discuss in section 3.3. The problem of convergence has been presented in section 3.4.

3.2. Construction of Eigen-Matrices

Before proceeding to study the equilibrium and the stability of the disk, one has to solve the transcendental equation (38) for prescribed values of the disk boundaries so as to evaluate the roots, k 's.

we have calculated the roots of the above mentioned transcendental equation, by dividing the problem into two sectors. First, to locate the points where $F(k)=0$ changes the sign and finding the zero's as accurately as we desired by another programme. In principle, there is an infinite spectrum for k with a fixed disk boundary. However, it is sufficient to obtain the first 20 zero's, accurate up to the sixth place after the decimal, are given in the table (2.1).

3.2.1 The Matrix Elements

The matrix element in equation (49) are certain integrated quantities over the disk, with the integrands which are products of some Bessel functions and the equilibrium quantities like $\sigma_0(r)$, $B_{0r}(r)$, $B_{0z}(r)$ etc. The function $J_m(kr)$, are oscillatory in nature with the increasing number of modes in the interval(0, 1) for large values of k 's. Thus then oscillating nature of integrands increases as matrices, involving large number of zeros are considered. The integration of such highly oscillating integrand is not trivial and we have employed very accurate routines to obtain the results. We have used 10-point Gaussian quadrature for the evaluation of these finite integrals, which essentially form the eigen-matrix M . To ensure the convergence of these integrals, we divide the interval(0,1) of integration and carry out the integration in the segments, again by 10-point quadrature method. The integrals over the intervals are then summed up to yield the net values of the integrals in the interval(0,1) and compared with corresponding values earlier. The convergence scheme employed by us, can be described as follows:

$$I = \int_0^1 Q(x) dx$$

Which has to be evaluated. It can be written as:

$$\int_0^1 Q(x) dx = \int_0^{1/2} Q(x) dx + \int_{1/2}^1 Q(x) dx$$

Now, if

$$I_1 = \int_0^{1/2} Q(x) dx \quad ; \quad I_2 = \int_{1/2}^1 Q(x) dx$$

then,

$$\left| \frac{I - (I_1 + I_2)}{I_1 + I_2} \right| \leq 10^{-3}$$

If the above condition is satisfied, one says the integral converges up to 10^{-3} . While integrating, an in built convergence test was incorporated in the quadrature programme.

Most of the matrix element are of the form

$$\int_0^1 Q(x) \left[\int_0^x P(\xi) d\xi \right] dx$$

A programme QUAD (Numerical Recipes) was modified for the purpose with convergence of both the integrands separately tested.

3.2.2. Generation of Eigen Patterns

Patterns associated with the eigenmodes of oscillation have been constructed by using a grid with 100 X 100. A 100 X 100 grid has been superimposed over the disk. Any

perturbed quantities, e.g. the radial component of perturbed magnetic field, may be obtained from

$$\tilde{b}_r(r, \varphi, t) = \text{Re} \left[\tilde{b}_r(r) e^{i(\omega t - m\varphi)} \right] \quad (3.2.1)$$

for a given eigen-frequency ω_j (3.2.1), and azimuthal wave number m . The radial part of the perturbation, $\tilde{b}_r(r)$ is calculated from the eigenfunctions $D_j^{(k)}$ and $E_j^{(k)}$ corresponding to ω_j as

$$\tilde{b}_r(r) = \frac{2}{2} \sum_{k=0}^{\infty} k \left\{ D_j^k J_{m+1}(kr) + E_j^k J_{m-1}(kr) \right\} \quad n_t = 5 * n \quad (3.2.2)$$

where eigenfunctions D_j^k and $E_j^{(k)}$ are complex. Eigenfrequency, ω_j , hence, introduces a radial phase in equation (3.2.1). At a given instant of time, t (say $t=0$), one can evaluate the perturbed magnetic field at all the mesh points. From the calculated values of $\tilde{b}_r(r, \varphi)$ at 100 X 100 grid, the perturbations over the disk have been plotted with an arbitrary scale of amplitude.

3.3. The Eigen Routine

The matrices in the eigenvalue problems are complex, infinite dimensional and non-symmetric.

The determination of the eigenvalue and eigenfunctions have been carried out by using the EISPACK interactive routines (numerical recipes, 1988). The interactive part of the programme has been developed by Dr. B.R. Sitaram of PRL.

3.4. Convergence of Eigenvalues and Eigenfunctions

Matrices of successively increasing dimension have been used to carry out the numerical accuracy of the eigenvalue-eigenfunctions. Eigenvalues generally depend on the value of the dimension $n_t + 5 * n$ (where n is the term retained in expansions for perturbed quantities), of the eigenmatrix and they do not converge to certain values when n_t is increased. As n is increased, the number of complex conjugate pairs and modes increases. Thus new modes of oscillations appear, while the values of the already existing modes are refined. The truncation of the eigenmatrix to a size n_t thus, contains modes upto $(n-1)$ modes only. The eigen modes of perturbations with much shorter wavelengths would be omitted by the truncation of M . From figures (3.1) and (3.2) we note that with progressive increase in the dimension of the eigenmatrix, the variations in the unstable eigenfrequencies in w -plane diminishes. However, the convergence is rather slow. The eigen routine tends to show numerical errors for very large matrices (75 x 75), hence the convergence of the eigenvalues can not be pursued indefinitely. We have used a maximum dimension of 60 X 60 on most of our calculations.

Referring to figures (3.1) and (3.2) which compare the eigenpatterns obtained by using 75 X 75 and 60 X 60 matrices, it is evident that for the eigenvalues, under

consideration, the eigen-contours and eigen-patterns do not exhibit any major variations. The convergence of the principle mode (or the dominant mode) can be seen in the table (2.2). Finally, we may remark again that the check on the convergence of various eigenvalues and eigenfunctions is very important, before a particular mode can be assumed a genuine mode of oscillation in a global problem.

Omega Real VS. Omega Im ($m=1$)

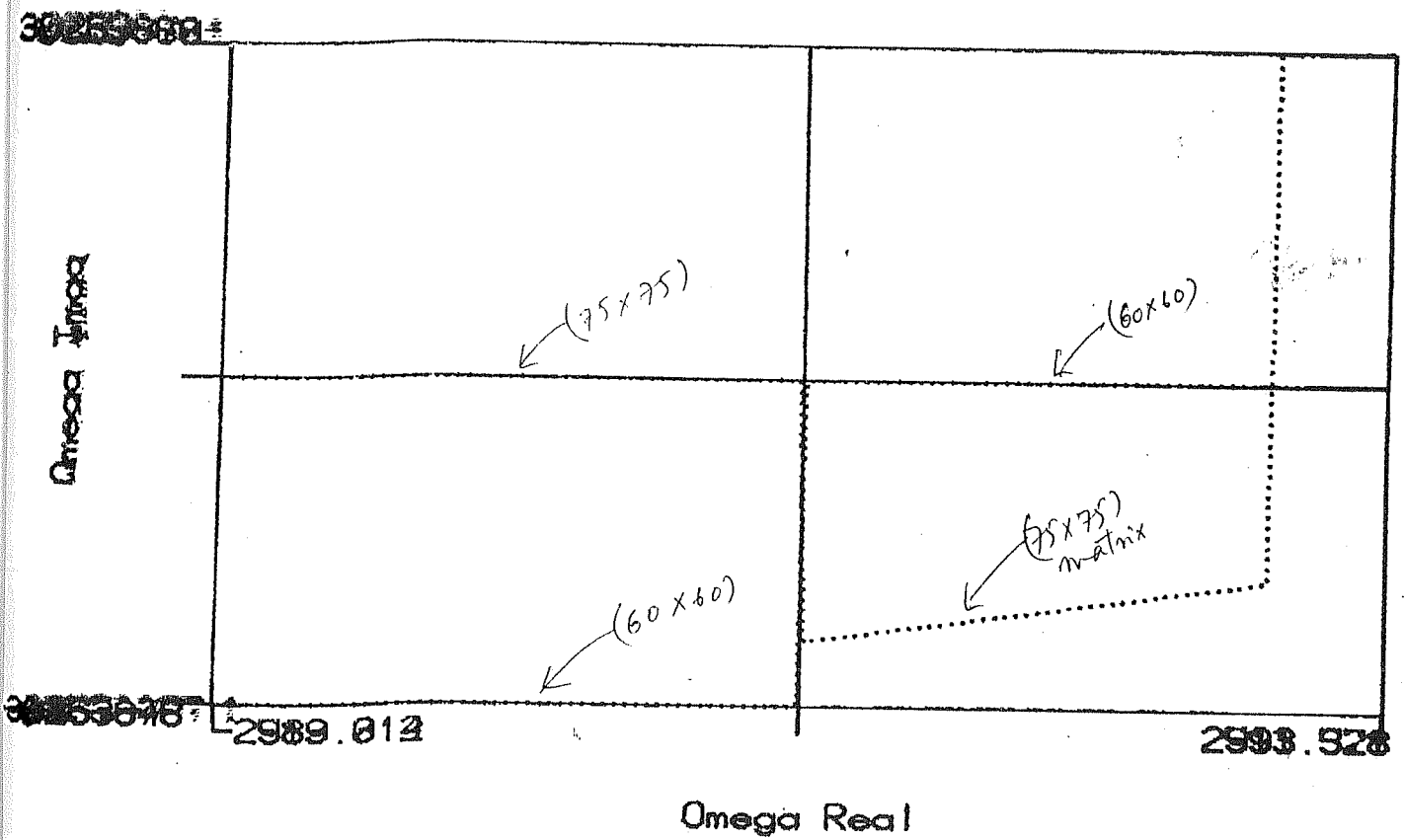


(Fig. 3.1)

Omega Real vs. Omega Imaginary ($m=2$)

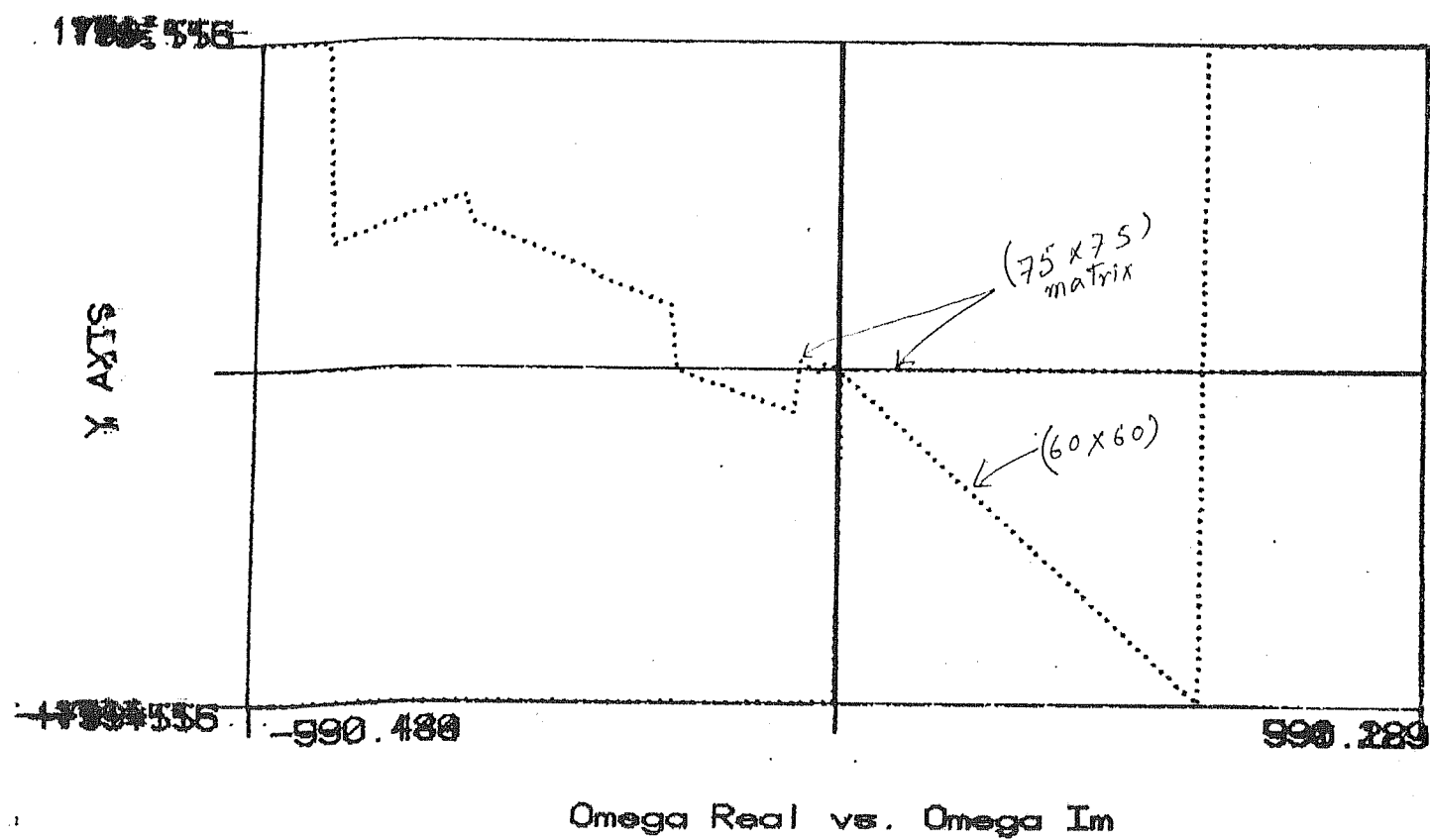


Fig (3.2)

CHAPTER IV

EPILOGUE

One of the most striking morphological features of the magnetic field of the spiral galaxies is their bisymmetric spiral structure. The BSS structure turns out to be the outcome of the dynamics of the system, namely, the interaction between the magnetic field and ionized component of the disk.

The dynamo theories, as proposed by Sofue et. al., Baryshnikova et. al., are not self-consistent and face several shortcomings as already described in Chapter I. An attempt has been made here to understand the full content of a self-consistent, boundary value problem, for a thin,

magnetized, gravitating disk in a one component ionized component) fluid model. In general, one should as well consider the neutral component and its interaction with ionized component via ambipolar drag. However, we have confined our study to one fluid model for simplicity. The problem is posed in an eigen-value form and the discrete spectrum of allowed modes has been obtained for different modes. In principle, infinite number of unstable modes are permissible in the gravitating magnetized disk. Unstable mode exhibits bisymmetric spiral features. These bisymmetric spirals occur as a natural consequence of the collective effects in the magnetized gravitating disk and thus explain the "problem of the origin" of BSS in the disk galaxies. The "persistence problem" which requires the amplification of the perturbation is also explained since the BSS are allowed for complex eigenmodes.

The growth rate for $m=1$ mode is larger than growth rate for $m=2$, and hence we see in galaxies mostly BSS structure. One should carry out the similar analysis for axisymmetric mode also, which perhaps should settle the question of $m=1$ dominance in the galaxies.

Eigenvalues with large-growth rate occur in the problem. In fact, in many small wavelength modes, $\omega_i > \omega_r$ and thus these represent violent instabilities in the system. Such explosive mode cannot grow indefinitely in the disk, since the energy reservoir is finite. Their evolution and saturation should be studied through a nonlinear calculation.

We would like to remark here that the eigenvalue problem, in the form discussed above, removes several difficulties encountered by the dynamo theories. However, one should also take into consideration the neutral component of the gas and a more complete analysis should include two component fluid equations - one for ionized one and the other for the neutral. Also, the analysis should be carried out for a thick disk. We have considered a thin magnetized gravitating disk. Gravity should also be considered in the subsequent analysis self-consistently. Lastly, a full analysis of the problem, requires a non-linear analysis of the evolution of the system. So far, no attempt has been made in this direction. Such a study is important to understand the secular transport of the energy in the system.

The problem of the dynamics and stability of a magnetized gravitating disk galaxies is extremely exciting and needs much work in future in order to understand many yet unsolved problems e.g. the cause of the dominance of bisymmetric spiral in the galaxies, the origin of the magnetic field, etc.

References

1. Baryshnikova et. al., 1987; Astron. Astrophys. 177, 27.
2. Beck, R. 1982, Astron. Astrophys. 106, 121.
3. Chandrasekhar, S. and Fermi, E., 1953, Ap. J. 241, 114.
4. Chandrasekhar, S. and Fermi, E., 1953, Ap. J. 241, 116.
5. Davis, L. and Greenstein, J.L., 1951, Ap. J. 206, 114.
6. Freedman, A.M. and Polyachenko, V.L., 1984, Physics of Gravitating Systems I, Equilibrium and Stability.
7. Fujimoto, M. and Sawa, T., 1986, Publ. Astron. Soc. Japan 32, 567.
8. Gilman, P., 1983, Ap. J. Supp. 53, 243.
9. Harrison, E.R., 1970, M.N.R.A.S., 147, 279.
10. Hiltner, W.A., 1949, Ap.J., 109, 471.
11. Hiltner, W.A., 1951, Ap.J., 114, 241.
12. Hosking, R.J., 1969, Austr. J. Phys. 22(4), 505.
13. Hoyle, F. and Ireland, J.G., 1961, M.N.R.A.S., 122, 35.
14. Hunter, C., 1972, Ann. Rev. Fluid Mech., 4, 219.
15. Kaplan, S.A. and Pikelner, S.B. 1970, Interstellar Medium,

Harvard University Press, Cambridge, Mass.

16. King, D.J., 1983, Mercury (March-April), 46.
17. Krashninnimova et. al., 1989, Astron. Astrophys. 213, 19.
18. Kulsrud, R.M., 1986, 'Plasma Astrophysics', Proceedings of the Joint Varenna-abastumani International School and Workshop, Sukhumi, USSR, 531.
19. Lin, C.C. and Shu, F.H., 1964, Ap.J. 140, 646.
20. Moisewitch, B.L., 1966, Variational Principles, Wiley and Sons Ltd.
21. Nakamura, T., 1983, Prog. Theor. Phys. 70, 747.
22. Nakamura, T., 1984, Prog. Theor. Phys. 71, 212.
23. Norman, C.A., 1987, Proceedings of the Varenna Summer School, eds. J. Audouze and F. Meldriorri (Italian Physical Society).
24. Numerical Recipes, 1985, Cambridge University Press
25. Parker, E.N., 1971a, Ap. J., 163, 255.
26. Parker, E.N., 1971b, Ap. J., 166, 295.
27. Parker, E.N., 1979, Cosmic Magnetic Fields, Clarendon Press (Oxford).
28. Panofsky, W.K.H. and M. Phillips, 1964, Classical Electricity and Magnetism, Addison-Wesley, London.

29. Piddington, J.H., 1964, M.N.R.A.S., 128, 345.
30. Piddington, J.H., 1978, Astrophys. Space Sci., 59, 237.
31. Purcell, E.M. and Spitzer, L., 1971, Ap. J., 187, 191.
32. Ruzmaikin, A.A. and Sokoloff, D.D., 1979, Astron. Astrophys., 78, 1.
33. Ruzmaikin et. al., 1981, Sov. Astron., 25, 533.
34. Ruzmaikin et. al., 1985, Astron. Astrophys. 148, 335.
35. Ruzmaikin et. al., 1986, in Plasma Astrophysics, Proc. Varenna-abastumani Workshop, ESA Publ. SP-251, p. 539.
36. Ruzmaikin et. al., 1988, Nature, 336, 341.
37. Sawa, T. and Fujimoto, M., 1980, Publ. Astron. Soc. Japan, 32, 551.
38. Sawa, T. and Fujimoto, M., 1986, Publ. Astron. Soc. Japan, 38, 133.
39. Schmitz, F., 1987, Astron. Astrophys., 179, 167.
40. Smyrnov, V.I., 1964, A Course on Higher Mathematics, Vol. II, Pergamon Press, Oxford.
41. Sofue, Y. et. al., 1986, ann. Rev. Astron. Astrophys. 24, 459.
42. Sofue, Y. and Takano, T., 1981, Publ. Astron. Soc. Japan,

33,47.

43. Spitzer, L., Jr., 1942, Ap. J., 95, 329.
44. Spitzer, L., 1966, Diffuse Matter in Space, John Wiley and Sons, Inc.
45. Spitzer, L., 1978, Physical Processes in the Interstellar Medium, Wiley Interscience.
46. Vallee, T.R., 1980, Astron. Astrophys., 86, 251.
47. Vallee, J.R., 1984, Astron. Soc. Can., 78, 57.
48. Verschuur, G.C., 1974, in Galactic and Extragalactic Radio Astronomy, ed. Verschuur and Kellerman, Springer-Verlag, chapter 8.
49. Verschuur, G.C., 1979, Fundamentals of Cosmic Physics, 5, 113.
50. Yobushita, S., 1969, M.N.R.A.S., 142, 201.
51. Zeldovich, et. al., 1983, Magnetic Fields in Astrophysics, Gordon and Breach Science Publishers.